Comparing Differentiated Rod And Cone Transcriptomes Reveals Rax As A Controller Of A Defined Cone Gene Regulatory Program

Thesis

Nicola de Prisco, M.Sc.

Comparing differentiated rod and cone transcriptomes reveals Rax as a controller of a defined cone gene regulatory program

Ph.D. Thesis

The Open University

Telethon Institute of Genetics and Medicine (TIGEM)

Director of Studies: Enrico Maria Surace, DVM

External Supervisor: Didier Trono, Ph.D.

Graphical Abstract

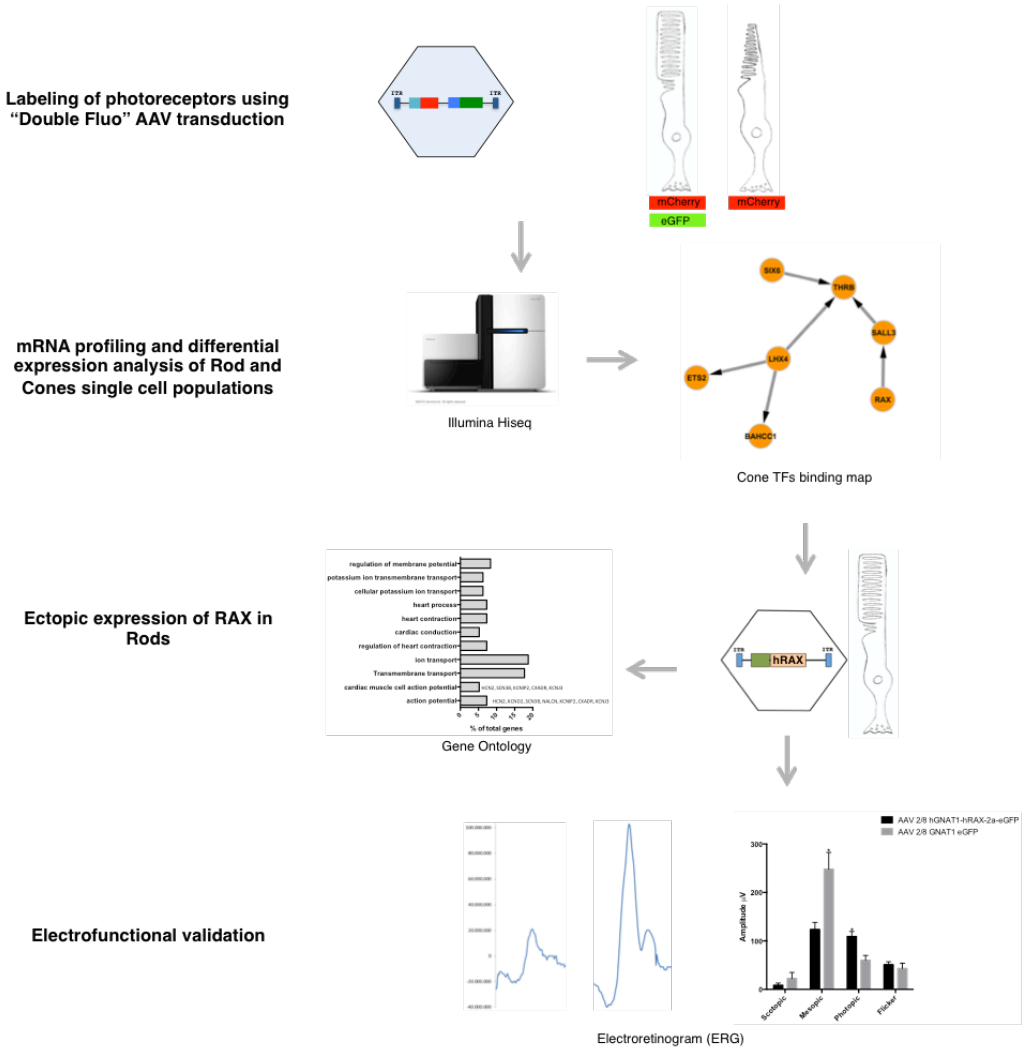

Highlights

- "Double Fluo" strategy enables the simultaneous and differential labeling of rods and cones
- Cone and rod differential expression showed eight rod and cone specific differentially expressed TFs transcription factors
- RAX, SALL3 and SIX6 form a putative regulatory network co-controlling many genes, including the key M-opsin TF drivers Thyroid Hormone Receptor Beta
- RAX mis-expression in rods determine an up-regulation in genes related to action potential
- Rods mis-expression of cone-specific TF, RAX, determine an up regulation of genes physiologically expressed in cones such as cone alfa transducin 2 (GNAT2)
- Retinae transduced with RAX showed a perturbed electrophysiological response, consistent with molecular findings

List of Abbreviations	
11-*cis*-retinal	11cRAL
Adeno associated viral vector	AAV
all-*trans*-retinal	atRAL
Biological processes	BP
cGMP-gated cation channels	CNG
Cone arrestin	CAR
Cone dystrophy	CD
Cone-rod dystrophy	CRD
Cone-Rod Homeobox	CRX
CRISPR-inactive CAS9	dCAS9
Differential expressed gene	DEG
Differential expression analysis	DEA
Electroretinography	ERG
Estrogen Related Receptor Beta	ESRRB
Expressed sequence tag	EST
G-protein coupled receptor Kinase 1	GRK1
Gene ontology	GO
Gene regulatory network	GRN
Gene therapy	GT
genome copies	GC
Guanine Nucleotide Binding Protein Alpha Transducing 1	GNAT1
Guanine Nucleotide Binding Protein Alpha Transducing 2	GNAT2
Guanosine diphosphate	GDP
guanosine triphosphate	GTP
Guanylate cyclase	GC
Guanylate cyclase activating protein	GCAP
Inherited retinal degenerative disease	IRDD

Inner nuclear layer	INL
Inner plexiform layer	IPL
Inverted terminal repeats	ITR
Ion channel family of hyperpolarization-activated cyclic nucleotide-gated	HCN
Leber congenital amaurosis	LCA
Medium wavelength cone opsin	OPN1Mw
Molecular function	MF
Neural retina leucin zipper	NRL
Non-human primates	NHP
Nuclear orphan receptor	NR2E3
Orthodenticle Homeobox 2	OTX2
Outer limiting membrane	OLM
Outer nuclear layer	ONL
Outer plexiform layer	OPL
Phosphodiesterase	PDE6
Photoreceptor	PR
Poly-adenylation signal	pA
Principal component analysis	PCA
recombinant AAV genome	rAAV
Retina And Anterior Neural Fold Homeobox	RAX
Retinal pigment epithelium	RPE
Retinal progenitor cell	RPC
Retinitis pigmentosa	RP
Rhodopsin	RHO
Rhodopsin kinase	RHOK
RNA sequencing	RNA-seq
Serial analysis of gene expression	SAGE

Short wavelength cone opsin	OPN1Sw
Thyroid Hormone receptor beta	THRb
Transcription factor	TF
transcription factor DP1	TFDP1
Visual System Homeobox 2	VSX2

Table of Content

Abstract

Purpose

Rods and cones convert light stimuli into signaling information for brain-mediated visual perception. Specific gene mutations primarily affecting both photoreceptor (PRs) types lead to retinal dystrophies, including rod-cone (retinitis pigmentosa) and cone-rod degeneration. Rods and cones are generated from common precursor cells and their differentiation program is strongly regulated by transcription factors (TFs) that control gene networks during development transitions and in the adult to maintain their identity and function.

The aim of this thesis was to investigate post-mitotic transcriptional regulation of rod- and cone-specific gene regulatory networks (GRNs). Specifically, retrieving transcription factor sets has biological relevance and may be instrumental for designing somatic gene transfer methodologies for both gene-based and regenerative therapeutic strategies.

Methods

We developed an Adeno-associated viral (AAV) vector-based transfer method to isolate rods and cones by fluorescence-based sorting. To isolate “pure” rod and cone populations from the same retinal samples we designed a double expression cassette (“double fluo”) encoding mCherry under the transcriptional control of the human G-protein coupled receptor Kinase 1 (GRK1) gene rods and cones-specific promoter elements of, and eGFP under the transcriptional control of rod-specific human Guanine Nucleotide Binding Protein Alpha Transducing (GNAT1) promoter elements. Porcine (*Sus* scrofa) retinae were injected with AAV 2/8 GRK1-mCherry_hGNAT1-eGFP, at the dose of $1x10^{12}$ genome copies (GC) per eye (n=3). The animals were sacrificed 15 days after injection to evaluate fluorescence reporter based rod and cone photoreceptor identities by histological and FACS analysis. We evaluated, on sorted populations, rods and cone specific transcriptomes by RNA sequencing (RNA-seq) using Illumina Hiseq 1500 (n=3). Moreover, after overexpression of human Retina And Anterior Neural Fold Homeobox (RAX), using subretinal injection of AAV2/8 hGNAT1-hRAX2aeGFP at a dose of 5 x 10^{11}gc/eye we studied the GRN associated with RAX, by a second round of RNA-seq. Electroretinography (ERG) was used to correlate RAX-specific GRN with retina function.

Results

Histological analysis showed unambiguous expression of both mCherry and eGFP in rods, whereas cones showed exclusive expression of mCherry. Furthermore, cone arrestin (CAR) showed exclusive co-localization with the

mCherry signal (cones), which was absent in red-green cells (rods). Photoreceptors specifically labeled were positive for both mCherry and eGFP (rods) or mCherry-only (cones) expressing Rhodopsin (RHO), Neural retina leucin zipper (NRL), Guanine Nucleotide Binding Protein Alpha Transducine 1 (GNAT1) (rod markers) and Short wavelength cone opsin (S-opsin), Medium wavelength cone opsin (M-opsin), Guanine Nucleotide Binding Protein Alpha Transducing 2 (GNAT2) (cone markers), respectively.

RNA-seq differential expression analysis (DEA) showed 198 differential expressed genes (DEGs), of which 68 genes were up-regulated and 128 genes down-regulated in rod versus cone analysis. Furthermore, 8 TFs were found differentially expressed in rods and 8 in cones. In the cone-specific TFs set, out of 3 known TFs (Rax, Sall3 and Six6), Rax was selected for further analysis. Rax was ectopically expressed in rods (Rax-rod) to reconstruct its GRN. Differential expression analysis identified 386 DEGs, of which 224 genes (58%) were up- and 162 (42%) down regulated. Clustering for biological processes gene ontology (BP-GO), showed enrichment in action potential genes. Furthermore, ERG showed a different light response of the hRax-treated retina. In particular, a decrease of the mesopic (dark adapted) and an increase of the photopic (light adapted) responses were found.

Conclusion

We showed that the “double fluo” provided a robust method to isolate and cross-compare rod and cone photoreceptors in the adult porcine retina upon photoreceptor somatic gene transfer via AAV vectors. Furthermore, RNA-seq data set analysis showed that the cone and rod specific transcriptome differs quantitatively by about 200 transcripts and that 8 TFs are photoreceptor specific In addition, the data show that post-mitotic rods are able to express cone genes upon Rax ectopic expression. Furthermore the data support a role of Rax in controlling cone-specific action potential gene set.

Introduction

Chapter 1. The organization of the retina and visual system

The visual system is the part of the central nervous system which gives organisms the ability to process visual detail, as well as enabling the formation of several non-image photo response functions (London *et al*, 2013). The visual system in animals allows individuals to assimilate information from their surroundings. The structure of the human eye can be divided into three main layers or tunics whose names reflect their basic functions: the fibrous, the vascular, and the nervous tunics (Figure 1)

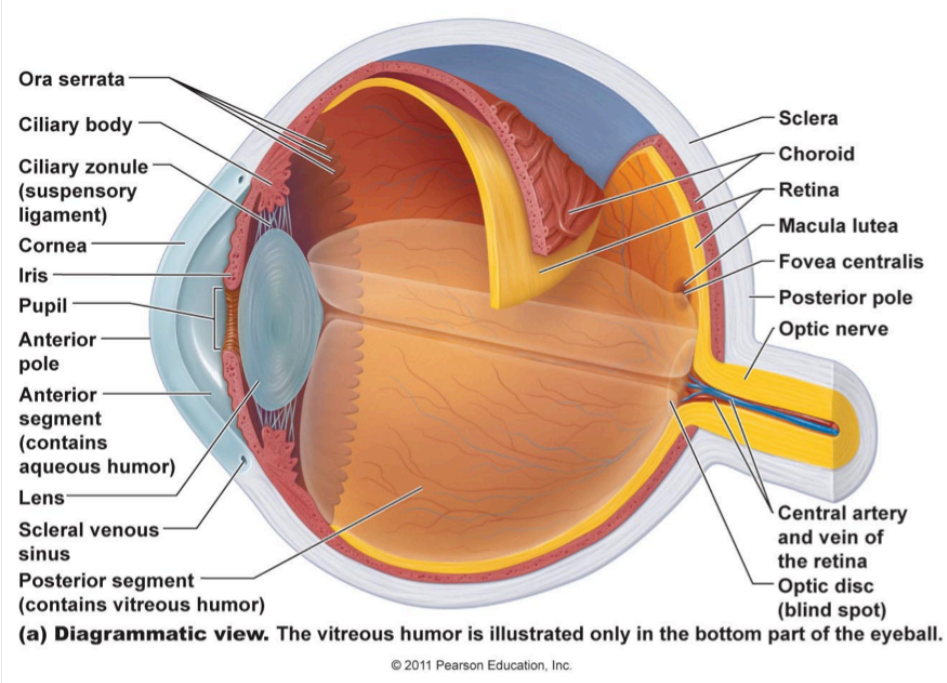

Figure 1 Schematic representation of human eye

The **fibrous tunic**, also known as the *tunica fibrosa oculi*, is the outer layer of the eyeball consisting of the cornea and sclera. It consists of dense connective

tissue filled with the collagen to both protect the inner components of the eye and maintain its shape. The **vascular tunic**, also known as the *tunica vasculosa oculi*, is the middle vascularized layer, which includes the iris, ciliary body, and choroids. The iris sits between the anterior chamber, which contains the aqueous humour essential for nourishing the lens and the cornea, and the posterior chamber filled with the vitreous humour. This substance is jelly-like and, besides helping the eye to keep its shape, it transmits the light to the back of the eye. Moreover, this fluid is enriched with anti-inflammatory and immunoregulatory mediators that is reminiscent of the cerebrospinal fluid that circulates around brain and spinal cord parenchymas (London *et al*, 2013). The lens is a clear, flexible structure responsible for sharpening of the image at the retina and it is connected to the ciliary body (which contains the ciliary muscles). The choroid contains blood vessels that supply the retinal cells with necessary oxygen and remove the waste products of respiration. The **nervous tunic**, also known as the *tunica nervosa oculi*, is the inner sensory structure, which includes the retina.

In this complex system, the act of seeing starts when the cornea and then the lens of the eye focuses an image of its surroundings onto the light-sensitive portion in the back of the eye. This photosensitive tissue serves as a transducer for the conversion of patterns of light into neuronal signals that travel through the optic nerve to reach the visual cortex where the perception is built.

1.1. Retina

The vertebrate retina has a highly organized and conserved structure. It acts as a miniaturized parallel processor with many different cell types dedicated to the extraction of useful features from the visual scene (Cepko, 2014) (Figure 2).

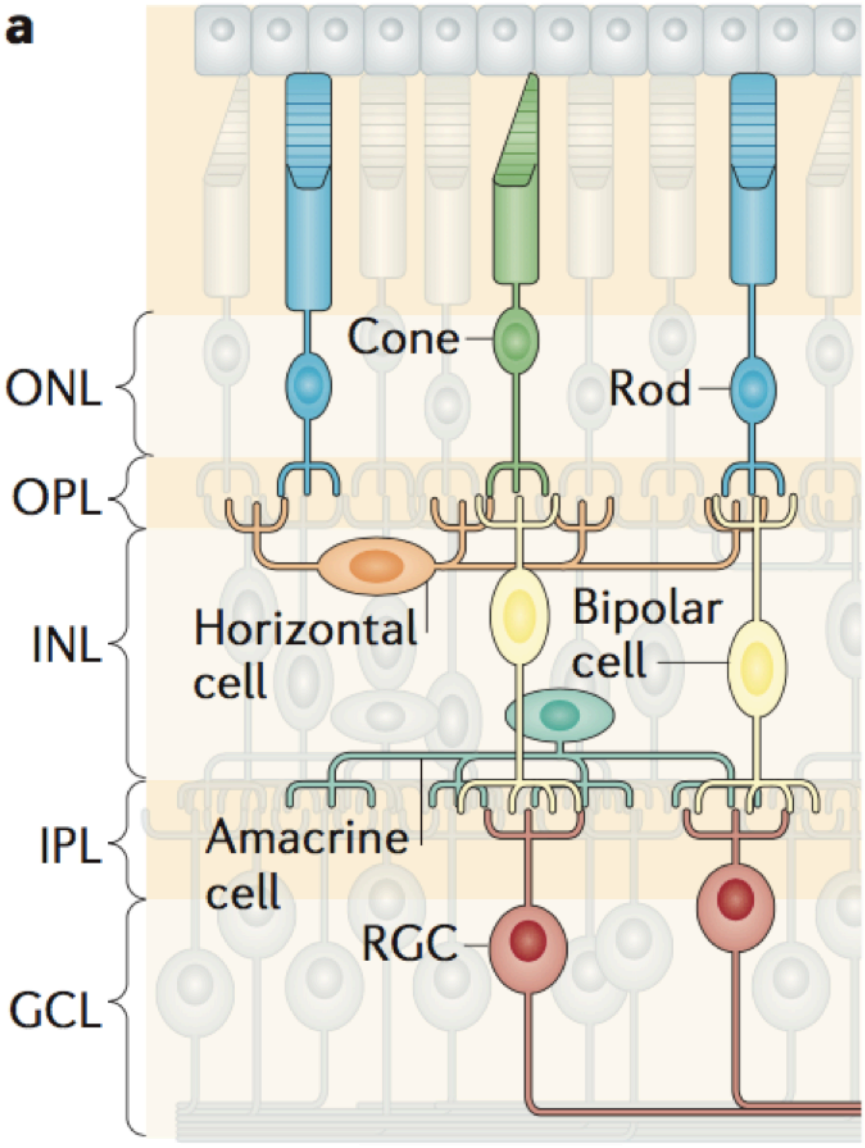

Figure 2. Mammalian retina structured as interconnected network of different cell types. From (Goldman, 2014)

The transformation of light stimulus into a nervous signal is carried out by more than 60 retinal cell types (Masland, 2012) divided into 6 different classes organized in three layers of nerve cell bodies and two of synapses forming an intricate neural network (Figure 2). The outer nuclear layer (ONL) contains cell bodies of the photoreceptors, rods and cones. The inner nuclear layer (INL) contains cell bodies of the bipolar, horizontal and amacrine cells whereas in the third layer ganglion cells and displaced amacrine cells are present. Dividing these nerve cell layers are two neutrophils where synaptic contacts occur: the outer plexiform layer (OPL) and the inner plexiform layer (IPL). In the OPL connections between rod and cones, vertically running bipolar cells and horizontally oriented horizontal cells occur; in the IPL connections between bipolar and ganglion cells are integrated by horizontal connection of amacrine cells. The most outer layer is the retinal pigment epithelium (RPE), which is situated between the choroid and the photoreceptors. The RPE nourishes the retina and is involved in the phagocytosis of the outer segment of photoreceptor cells and is also involved in the chromophore regeneration.

Muller glia are the only cell type that span all retinal layers and have processes that contact neighboring neurons and form part of the outer and inner limiting membranes. They function as barriers and conduits regulating the homeostasis of a wide range of molecules between different retinal cells and compartments (Franze *et al*, 2007).

1.2. Rods and Cones

All cells in the retina, including rods and cones, are derived from retinal progenitor cells (RPCs) (Cepko, 2014). Photoreceptors are the first point of contact between the outside world and the central nervous system.

PRs convert light into chemical signals that can stimulate biological processes triggering the cascade of biochemical events terminating in image formation in the brain.

Two kinds of PRs developed during evolution: the ciliary or c-type and the rhabdomeric or r-type (Morshedian *et al*, 2017), the former very common in vertebrates and the latter in invertebrate phyla. Although ciliary photoreceptors are found in many phyla, vertebrates seem to be unique in having two distinct kinds of PRs, which together span the entire range of vision, from single photons to bright light. The rods in the mammalian retina are PRs able to respond to dim light while there are two or three type of cone cells, depending of the species, which can detect and discriminate colors. Cones are robust conical-shaped structures that have their cell bodies situated in a single row right below the outer limiting membrane (OLM) and their inner and outer segments protruding into the subretinal space towards the pigment epithelium (Figure 3).

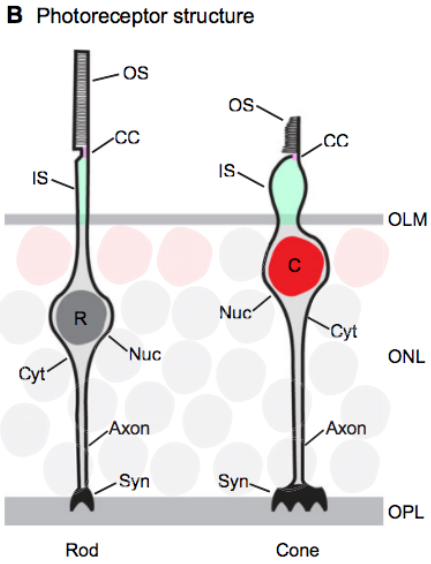

Figure 3 Rod and Cone

Photoreceptors exhibit a highly polarized structure. The outer segment (OS), a modified primary cilium has membrane discs (in rods) and folds (in cones), structures specialized to capture light. The inner segment (IS), is specialized area of cytoplasm starting at the outer limiting membrane (OLM) of the retina. It is a site of elevated protein biosynthesis, and the resulting products are transported through the narrow connecting cilium (CC, in pink) into the OS. Photoreceptors span the ONL and extend their axons to the outer plexiform layer (OPL), where they form synapses (Syn) with horizontal and bipolar interneurons. Cones exhibit large multisynaptic pedicles, whereas rods have a smaller synaptic spherule. From (Brzezinski & Reh, 2015)

The fovea is an anatomical region of the retina in human and non-human primates (NHP) where only cones are present. This region has a role in visual acuity. In higher mammals such as humans there are different type of cones, detecting long, medium and short wavelength (L- M- S-cone). The absorbance spectrum of cones is due to differential expression of phototransduction opsin proteins (S-, M- and L-opsins). Rods, on the other hand, are slim rod-shaped structures with their inner and outer segments filling the area between the larger cones in the subretinal space and stretching to the pigment epithelium cells. Rod cell bodies make up the remainder of the outer nuclear layer below the

cone cell bodies. Rods are crucial for the detection of dim light and for peripheral vision. This characteristic is due to the abundant expression of Rho, a photo-protein localized on the discs that, similarly to cone opsins, triggers the photo transduction cascade.

The photoreceptor cell structure of rods and cones is similar and consists of 1) an outer segment, filled with stacks of membranes containing the visual pigment molecules such as rhodopsin, 2) an inner segment containing mitochondria, ribosomes and membranes where opsin molecules are assembled and transferred to the outer segment discs 3) a cell body containing the nucleus of the photoreceptor cell and 4) a synaptic terminal where neurotransmission to second order neurons occurs.

Apical processes from the pigment epithelium envelope the outer segments of both rods and cones. The apical portion of PRs (outer segment) is efficiently renewed by receptor-mediated phagocytosis in a diurnal rhythm coordinated by RPE cells. This phenomenon is crucial both for long-term viability and functionality of photoreceptors (Young, 1967).

Morphological difference between mammalian cones and rods are related to the structure of the outer segment membrane. In cones, the entire membrane is continuous with the plasma membrane of the inner segment, whereas in rods the bulk of the outer segment membrane is sealed off from the plasma membrane in the form of discs that resemble deflated balloons (Figure 3).

Despite the morphological differences between mammal PRs, the light response properties of cone and rod photoreceptors are remarkably similar to

each other but they exhibit a few major differences: the defining feature in the response of the rod photoreceptor is its ability, under dark-adapted conditions, to respond reliably (i.e. with good signal-to-noise ratio) to the absorption of individual photons of light. Cone photoreceptors have the ability i) to respond rapidly, ii) to function over an enormous range of intensities, iii) never saturate in steady light, independently of the intensity and iv) the ability to recover much of their responsiveness almost instantaneously when an intense light is extinguished (Lamb, 2013). Furthermore, cone synapses are connected to more cone bipolar cells while there is a one-to-one connection between rod and rod bipolar cells (Masland, 2012).

1.3. Phototransduction pathway: from photoreceptors to visual cortex

Rods and cones have well-defined response properties. Rods are characterized by high sensitivity, slow response and slow dark adaptation, whereas cones have low sensitivity, fast response and fast dark adaptation (Shichida & Matsuyama, 2009). Both PRs share the signaling pathway of phototransduction. Rod phototransduction has been more comprehensively studied than that in cones (Figure 4). It takes place in the rod OS discs with the absorption of light by Rho. Rho binds to the light-sensitive chromophore 11-*cis*-retinal (11cRAL), a derivative of vitamin A (Nathans, 1992). The phototransduction cascade initiates when the visual pigment, rhodopsin, absorbs a photon that induces a

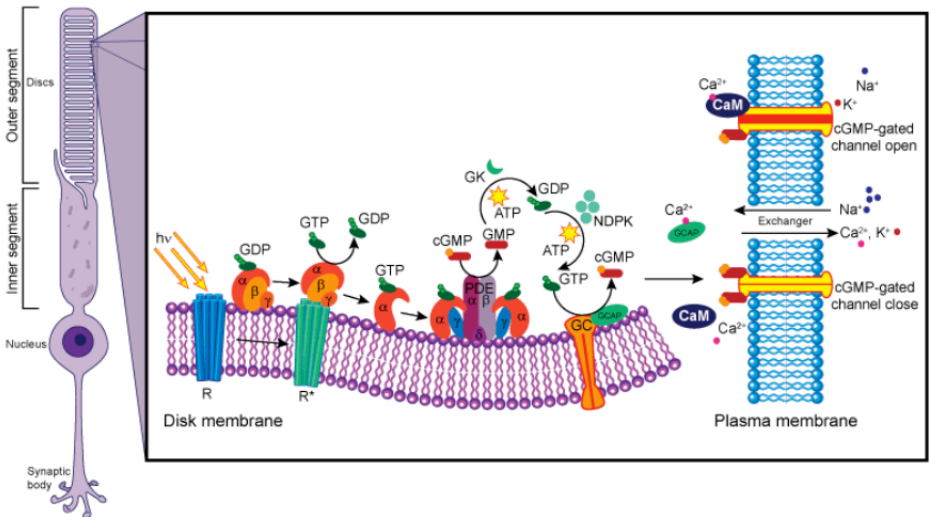

Figure 2. Phototransduction pathway in rod PRs

R: rhodopsin; R*: photoactivated rhodopsin; PDE6: phosphodiesterase 6; GCAP: guanylate cyclase activating protein; GC: guanylate cyclase. From http://mutagenetix.utsouthwestern.edu/phenotypic/phenotypic_rec.cfm?pk=282

conformational change of the chromophore to all-*trans*, which still has the same

chemical structure as the *cis* but a different physical form. Because the all-*trans*-retinal (atRAL) no longer fits with the rhodopsin, it begins to pull away from it until there is a complete split (within seconds). This in turn induces conformational changes and the activation of Rho, (R*). This intermediate molecule (metarhodopsin II) interacts with the next member of the cascade, a G-protein called Transducin (G), which is a heterotrimeric protein (αβγ). This interaction induces the subunit α of the transducin to exchange a bound guanosine diphosphate (GDP) moiety to guanosine triphosphate (GTP). The activated GTP-bounded subunit (G*α) detaches from the β and γ subunits of the transducin and associates with the next member of the cascade, the phosphodiesterase 6 (PDE6) which is a multisubunit complex composed of two tightly bound catalytic subunits, (99kDa, PDE) and (98kDa, PDE) in addition to two identical inhibitory subunits of 11kDa. The G*α subunit interacts directly with the inhibitory subunit of the γPDE6. An increase in the activity of the cGMP phosphodiesterase at this stage induces a fall in the concentration of cGMP in the cytoplasm (Nathans, 1992) which leads to the closure of cGMP-gated cation channels (CNG) with a consequent decline in calcium concentration within the cell. This causes a graded hyperpolarization of the plasma membrane. Hyperpolarization determines decrease glutamate released at the synaptic ribbon, this determine the transmission of the signal through bipolar cells to the optic nerve and to the brain. The decline in calcium concentration mediates the recovery of the photoreceptor cell after a bleach of light. This is as important for maintaining sensitivity in vision as the cell's ability to respond to a single photon.

Deactivation of rhodopsin starts with phosphorylation by rhodopsin kinase (RHOK) and is followed by the capture of rhodopsin by the protein arrestin (Dhallan *et al*, 1992). The arrestin binding prevents further activation of transducin and releases the all-*trans*-retinal from rhodopsin. The concentration of cGMP within the cell is restored by the increased synthesis of cGMP by a retinal guanylate cyclase (GC).

Notwithstanding that the rod phototransduction cascade has been more studied than that in cones, photoreceptor connections with the second neuron, bipolar cells, are well established. Cones connect to ON- and OFF-cone bipolar cells, which in turn connect to ON- and OFF-ganglion cells. The virtual direct connection between cone and ganglion cells through bipolar cells makes cones respond faster than rods. Otherwise two different pathways are used from rods to transmit the signal to the ganglion cells: i) Rod signals feed into both ON- and OFF-channels in the inner retina via rod bipolar and AII-amacrine cells, defining the primary rod pathway. ii) Rods are able to transmit signals via cone bipolar cells through gap junction connections with cones in the outer retina defining the secondary rod pathway (Feigenspan *et al*, 2004; Tsukamoto *et al*, 2001; Seeliger *et al*, 2011) (Figure 5).

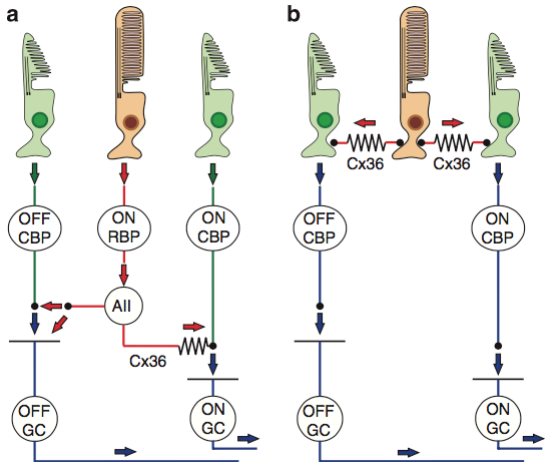

Figure 5 Schematic diagram of rod and cone pathways in the mammalian retina.

(A) Primary rod pathway: rod signals are converted via rod bipolar cell (ON-RBP) onto AII-amacrine cell. The AII provides electrical input via gap junctions containing Cx36 to ON-cone bipolar cells (ON-CBP) and via synapses into the OFF-pathway (OFF-cone bipolar cells, OFF-CBP and OFF ganglion cells, OFF-GC). (B) Secondary rod pathway: rods signals transmitted directly to cones via Cx36 containing gap junctions. From (Seeliger *et al*, 2011)

The reduction of synaptic activity due to closure of cGMP channels during response to light in PRs generates a detectable ERG signal during the early phase shortly after a light flash. The change in membrane potential is sensed by the ion channel family of hyperpolarization-activated cyclic nucleotide-gated (HCN) channel family, in particular by HCN1 (Seeliger *et al*, 2011). The HCNs cation channels comprises four members HCN1-4. Upon hyperpolarization, all four isoforms, following different kinetics, generate an inward current depolarizing the membrane (Ludwig *et al*, 1998; Santoro *et al*, 1998). The role of this class of proteins in brain and heart cells is to ensure a rhythmic activity of hyperpolarization-depolarization (Herrmann *et al*, 2015). Knop and colleagues in 2008 demonstrated that the light responses are considerably prolonged in a HCN1 KO mouse model (Knop *et al*, 2008). Furthermore, in 2011 Seeliger and

colleagues showed that the lack of HCN1 in mouse retina results in a sustained rod response and the saturation of the retinal network after bright light exposure resulting in a loss of downstream cone signaling (Seeliger *et al*, 2011)(Figure 6).

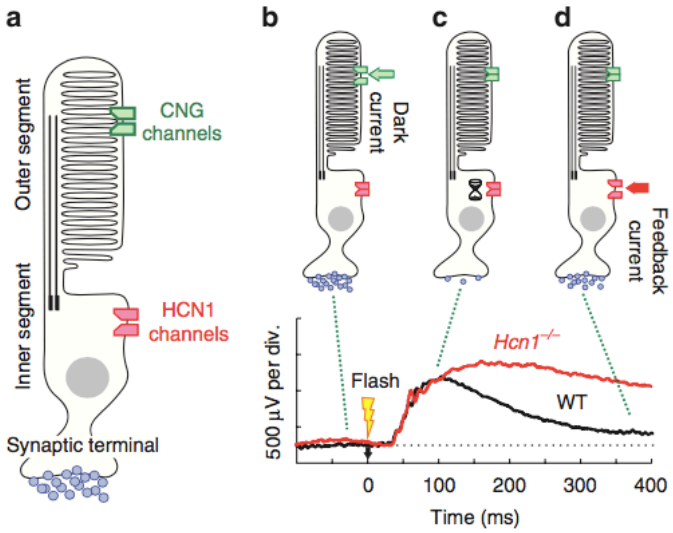

Figure 6 Role of HCN1 channels in photoreceptor signal generation

(A) Schematic sketch of a rod PR. Cyclic-nucleotide gated (CNG) and HCN1 channel are highlighted. (B-C-D) Scheme of the transitions between dark state to light responsive state. From (Seeliger *et al*, 2011)

Chapter 2. Photoreceptor development and homeostasis in the mammalian retina

2.1. From progenitors to photoreceptors, timing of photoreceptor genesis.

There is an evolutionarily conserved order for the genesis of the neurons and glia of the retina (Cepko, 2015). PRs are generated from a population of proliferative progenitor cells in the retinal neuroepithelium, a derivative of the neural tube. Rod and cone photoreceptors, along with all of the other retinal cell types, are generated from retinal multipotent progenitor cells (RPCs). These progenitor cells can divide both symmetrically and asymmetrically, and their terminal division can generate different retinal cell types (Brzezinski & Reh, 2015). In general, the first cone photoreceptors are formed before the initiation of rod photoreceptor production (Carter-Dawson & LaVail, 1979), (Figure 7 A-B)

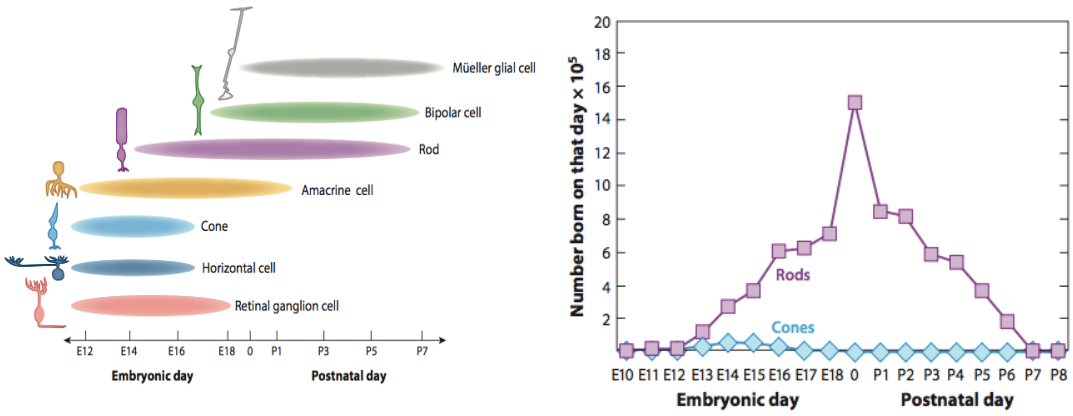

Figure 7 Timing of retinal cells genesis from (Cepko, 2015)

During the last 25 years, many tracing studies have demonstrated that RPCs are pluripotent and that these progenitors are not limited to producing a single

type of retinal neuron, i.e. there are no progenitors that are solely restricted to producing photoreceptors, but starting from RPCs through differential expression of regulators such as TFs, these cells can direct their fate into different retinal lineages (Turner & Cepko, 1987).

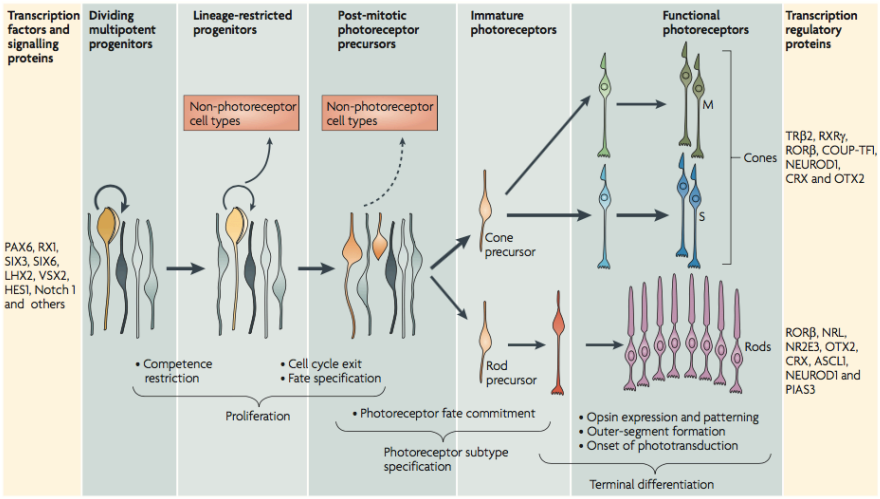

Figure 8 Stages of photoreceptor development reviewed by (Swaroop *et al*, 2010)

The process of photoreceptor development can be divided into five major steps: first, proliferation of multipotent RPCs; second, restriction of the competence of RPCs; third, cell fate specification and commitment to photoreceptor precursors during or after final mitosis; fourth, expression of photoreceptor genes, such as those for phototransduction and morphogenesis; and fifth, axonal growth, synapse formation and outer segment biogenesis (Figure 8) (Swaroop *et al*, 2010). The earliest steps in photoreceptor development involve signaling through the Notch receptor. High levels of Notch seem to maintain the cycling of progenitor cells, and inhibition of Notch drives progenitors to commit to the cone

or rod photoreceptor fate, depending on the developmental stage, over other cell fates.

2.2. Transcription factors in photoreceptor development and homeostasis

During the steps from the exit of RPCs from the cell cycle to adult and mature PRs, a plethora of TFs form an intricate GRN leading to the specification of rods, cones and all the retinal cells.

One of the key factors in PR development is Orthodenticle Homeobox 2 (Otx2). In the mouse retina, the expression level of Otx2 is up-regulated after RPC cell cycle exit. The expression of OTX2 can activate the expression of additional TFs such as Vsx2 and Prdm1. These TFs have the ability to lead the development of bipolar cells and photoreceptors, respectively (Figure 9) (Kim *et al*, 2008a).

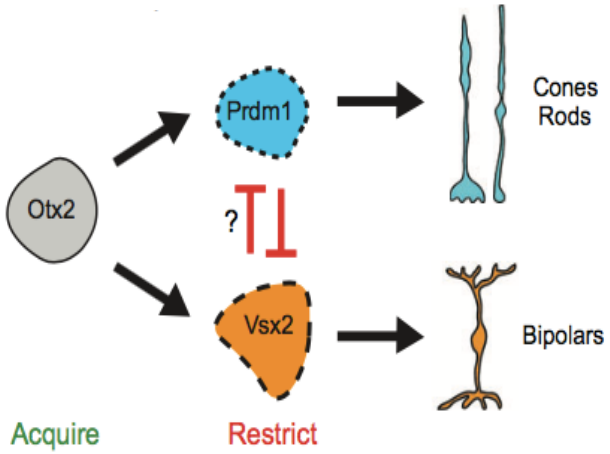

Figure 9 Otx 2 role in fate decision between PRs and bipolar cells

Otx2, in turn, activates the expression of Prdm1 and Vsx2, which may restrict bipolar and PRs potential respectively, from (Brzezinski & Reh, 2015)

Brezinsky and colleague in 2013 demonstrated that Prdm1 expressing cells can give rise to all of the retinal cells except ganglion cells (GCs) and Muller glia, demonstrating indirectly that Otx2 expression is a default program, and that this TF has to be repressed to generate other retinal cell types. The GRN involved in PR development begins with the loss of Notch expression driving the RPCs to cell cycle exit. Otx2 expression generates a cascade of relevant transcriptional events. First, Otx2 leads, together with Rorb, to the expression of Prdm1. Alternatively, Rorb and Foxn4 can cooperate to activate Ptf1a and push the cell towards amacrine or horizontal cell fates (Fujitani *et al*, 2006). Otx2 also activates the expression of Crx in all the PR cells. The distinction between rod and cone gene expression profiles occurs downstream (or independently) of Otx2 and Crx, and two key factors that control this specification event are Rorβ and Nrl (Swaroop *et al*, 2010). Otx2 and Rorβ are needed to initiate the expression of the transcription factor Nrl in a subpopulation of newly postmitotic precursors: these Nrl-expressing cells will develop into rod photoreceptors (Akimoto *et al*, 2006). Nrl is needed to activate several essential rod-specific genes, including Nr2e3, a transcription factor that can both co-activate rod genes and silence cone genes, such as Opn1sw (S-opsin), in rods. When Nrl is overexpressed using a Crx enhancer, only cones, and not bipolar cells, become reprogrammed to a rod fate (Oh *et al*, 2007), (Figure 10).

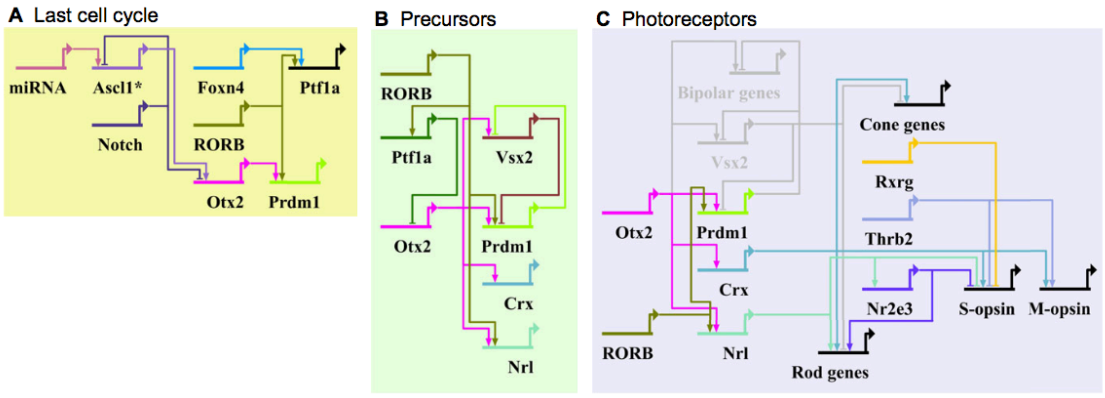

Figure 10 Gene regulatory networks involved in photoreceptor development from (Brzezinski & Reh, 2015)

Alternatively, in non-NRL expressing cells, Crx in combination with Trb2 can activate Opn1mw expression giving the specification of M-cones.

Since the rod GRN is well characterized, the most reliable model is the transcriptional dominance model proposed by Swaroop and colleague in 2010. This model includes three fundamental attributes: first, that all terminally differentiated photoreceptors originate from a common postmitotic photoreceptor precursor that has the potential to form rods or any of the cone subtypes; second, that a photoreceptor precursor cell follows a default pathway to differentiate into an s cone unless additional regulatory signals direct the precursor to acquire a rod or M cone identity; and third, that the acquisition of a specific fate by a photoreceptor precursor is established by a particular set of transcription-regulatory factors gaining dominance at a given developmental stage. These TFs (Otx2, Crx, Rorb, Nrl, Nr2e3 and Trb2) engage in a transcriptional contest for dominance that will ultimately determine the cells fate.

2.3. Neural retina leucine zipper (NRL) and Cone Rod homeobox (CRX)

Neural retina leucine zipper (NRL)

The decision to be or not to be a rod PR is largely determined by NRL, a neural transcription factor of the Maf subfamily. The Maf family is characterized by a typical bZip structure; these transcription factors act as important regulators of the development and differentiation of many organs and tissues including the retina. (Tsuchiya *et al*, 2015). The Maf family has two distinct subgroups of proteins categorized according to their molecular size into large and small Mafs. NRL is classified in the group of large Maf transcription factors that, differently from the small Mafs, have a transactivation domain and a typical bZip structure, which is a motif for protein dimerization and DNA binding (Fujiwara *et al*, 1993). In the mouse neural retina, NRL is exclusively expressed in rod photoreceptors from the embryonic stage E.12 (Akimoto *et al*, 2006) (Figure 11).

Because of the expression of NRL in RPCs, these cells restrict their fate decision becoming rods and expressing rhodopsin from 4-5 postnatal days.

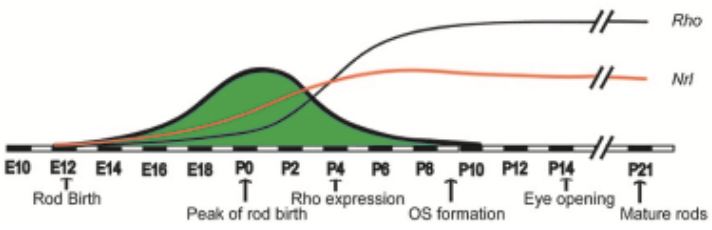

Figure 11 Rod birth timing and NRL expression during time from (Akimoto *et al*, 2006)

Montana et al. in 2010 showed that OTX2, CRX and RORb regulate NRL

expression. They proposed a model in which NRL expression is primarily initiated by OTX2 and RORb and later maintained at high levels by CRX and RORb (Montana *et al*, 2011). The high level of NRL expression in rods permits the activation of several rod genes and simultaneously represses cone genes in rods, either directly or by activating the downstream repressor *Nr2e3* (Oh et al., 2008; PENG & CHEN, 2005). The complete knock out of NRL (NRL $^{-/-}$) In mice fails to initiate rod gene expression, and rod precursors show a de-repression of cone genes, which results in a conversion of the cells into cones in the adult retina (Mears *et al*, 2001, 2015). Furthermore, NRL depletion in the adult retina via conditional K.O. showed a partial reprogramming of adult rods into cone-like cells, preventing retinal degeneration in Rho null mice (Montana *et al*, 2013).

Genetic studies of patients affected by retinitis pigmentosa (RP), an inherited form of retinal dystrophies, identified several missense mutations in the coding sequence of the NRL gene that causes a dominant form of RP. Mutations within the NRL gene are also associated with recessively inherited photoreceptor degeneration caused by an aberrant protein without a bZIP domain that is unable to bind the promoter sequences showing reduced transcriptional activation of the rhodopsin and of NRL regulated genes. (Jayaram *et al*, 2012).

Cone-Rod Homeobox (CRX)

Cone-Rod Homeobox, CRX, is a homeodomain transcription factor expressed from the embryonic day 12.5 in mouse retina and in adult PRs. In 1997 the groups of Cepko and Zack independently identified the OTX2-like factor CRX.

They found expression of CRX in both rod and cones and sustained expression also into the adult PRs. The high level expression of CRX has a crucial role in regulation of photoreceptor gene expression (Chen *et al*, 1997; Furukawa *et al*, 1997b). Furthermore, the expression of cone rod homeobox was also detected in pineal gland, regulating the expression of genes involved in synthesizing the circadian hormone melatonin in mice and in bipolar cells of the inner retina in mouse and human, demonstrating a potential function also in these cells (Wang *et al*, 2002).

Based on gene expression profile studies, Crx is a trans-activator for many photoreceptor genes. Crx alone has only a moderate transactivating activity even with the *rhodopsin* promoter, a well-known Crx target Chen et al., 1997). Thus, one mechanism for Crx to activate transcription is to interact with other transcription regulators including the photoreceptor-specific transcription factors Nrl and Nr2e3. In 2016 White and colleagues have revaluated the role of CRX as a transcriptional activator. They have demonstrated that the ability of CRX to activate or repress a gene strictly depends on: i) the number of CRX sites ii) the presence or absence of an NRL binding site. A low number of CRX binding sites is correlated with activation of gene expression; on the other hand a high number of binding sites is related to gene repression. This trend is overturned when many binding CRX binding sites are associated with the NRL binding site (White *et al*, 2016)

Due to its important role in the expression of photoreceptor genes in both rods and cones, CRX null mice (CRX $^{-/-}$) are blind at birth without detectable

photoreceptor function, resembling the phenotype of leber congenital amaurosis (LCA) (Furukawa *et al*, 1999).

Retina and anterior neural fold homeobox (RAX)

Nrl and *Crx* have an important involvement both in PRs development and maintenance of post mitotic PRs cells. Recently was shown that similarly *Rax* is important not only during the early steps of retinal and eye development but also in the maintenance of cone PRs in mouse (Irie *et al*, 2015).

Retina and anterior neural fold homeobox is a paired type homeobox gene, whose expression was first identified in the developing mouse retina (Mathers *et al*, 1997; Furukawa *et al*, 1997a). The encoded protein contains two characteristic domains conserved in homeo-domain proteins: an octapeptide motif in the N-terminus and an OAR domain in the C-terminus. The OAR domain is a 15-amino-acid sequence with a putative role in transactivation of gene expression (Furukawa *et al*, 1997a). Both the octapeptide motif and the OAR domain are evolutionary conserved among different species from *Drosophila melanogaster* to human (Muranishi *et al*, 2012) (Figure 12).

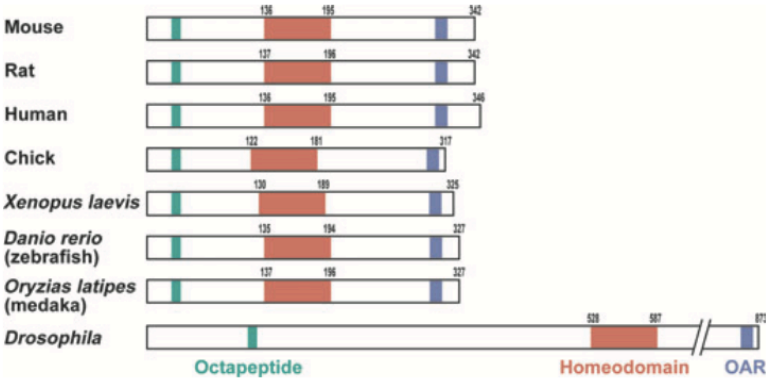

Figure 12 Evolutionary conservation of RAX protein

Schematic representation of putative domains of RAX protein, conserved from mouse to Drosophila. From (Muranishi *et al*, 2012)

During development of mouse embryos, Rax is expressed in the neuroepithelium of the retina and hypothalamus, at embryonic stage 9.5 (E9.5). Its expression is restricted to the optic vesicles and from E10.5 Rax expression is observed in the whole retinal region (Figure 13).

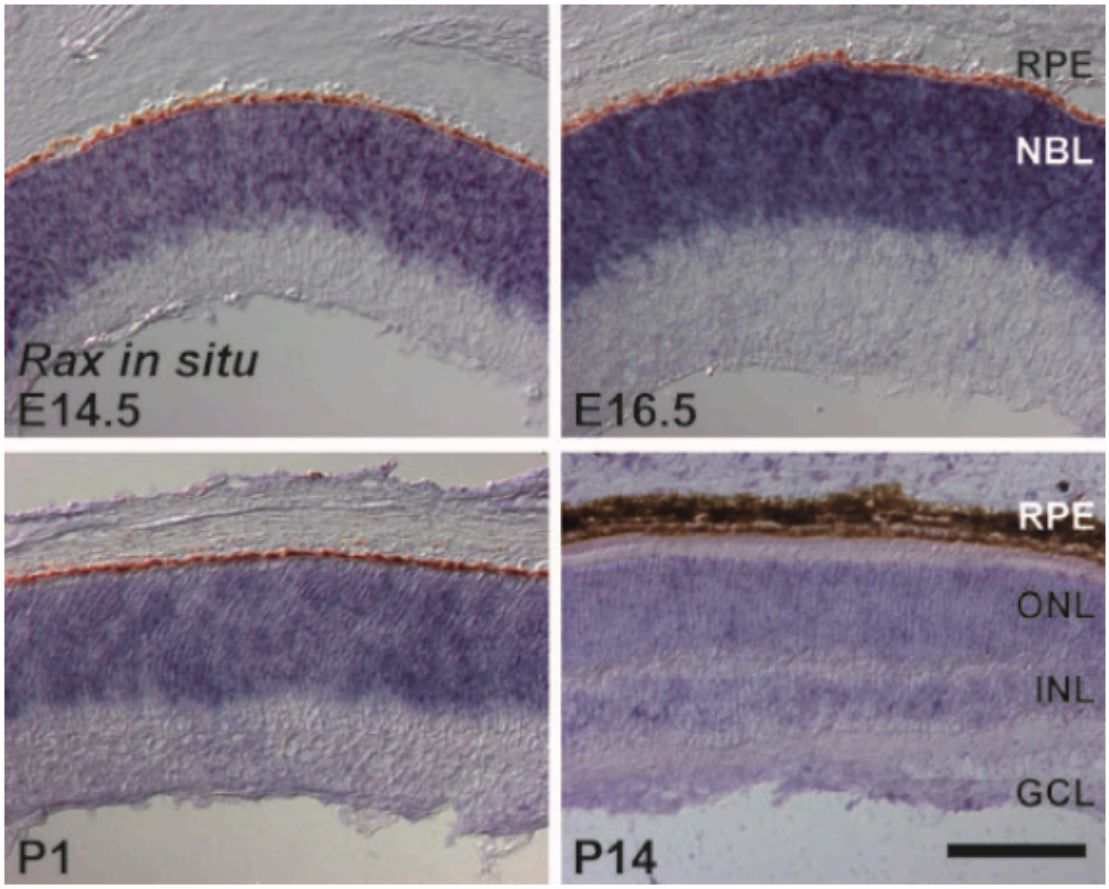

Figure 13 Rax expression in developing mouse retina

At embryonic day 14.5 (E14.5), Rax expression is restricted to the developing retina. At E16.5, Rax expression level reaches its highest level in retinal precursor cells, and then gradually decreases. The reduced Rax signal is observed at postnatal day 1 (P1) and P14 when retinal cell differentiation occurs. GCL, ganglion cell layer; INL, inner nuclear layer; NBL, neuroblastic layer (progenitor layer); ONL, outer nuclear layer (photoreceptor layer); RPE, retinal pigment epithelium. From (Muranishi *et al*, 2012).

After birth, Rax expression is limited to a few regions in the retina, including the progenitor layer, the photoreceptor precursor layer, and the inner nuclear layer. In adult mouse retina (P14-P21), Rax expression decreases and it is maintained basal into ONL and in Muller cells (Irie *et al*, 2015) (Figure 13-14).

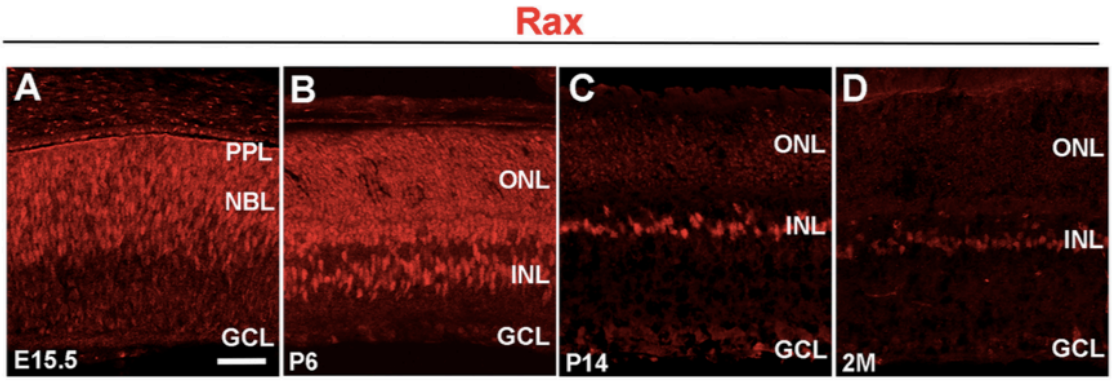

Figure 14 Expression of Rax in postnatal and adult mouse retina

(A to D) At E15.5 Rax is expressed in neuroblastic layer and in presumptive photoreceptor layer. P6 retina shows expression in ONL and INL; in adult the expression in restricted to ONL and muller cells in INL. NBL, neuroblastic layer; PPL, presumptive photoreceptor layer; ONL, outer nuclear layer; INL, inner nuclear layer; GCL, ganglion cell layer. From (Irie *et al*, 2015)

Several studies demonstrated that Rax is a key transcription factor for the formation of eyes in vertebrates. Rax-null mutant mice show reduced brain size and absence of the optic vesicles (Mathers *et al*, 1997). In humans, mutations of the RAX locus are associated with anophthalmia and microphthalmia (Bailey *et al*, 2004). Consistent with the role of Rax in mammals, the absence of the Rax protein in medaka and zebrafish causes non-development or loss of the eye, respectively. On the other hand, overexpression of Rax in Xenopus and zebrafish embryos leads to over proliferation of retinal cells (Terada *et al*, 2006).

Otx2 was reported to be a master regulator of PR fate determination. An approximately 500 bp cis-regulatory region, named “EELPOT”, is responsible for Otx2 expression in photoreceptor precursors. EELPOT in vivo binding of Rax was demonstrated in embryonic mouse retina extract and in vitro luciferase transactivation was reported. In addition, the expression of Otx2 decreased

remarkably in the retina of PRs precursor-specific Rax CKO mice, indicating that Rax directly regulates Otx2 transcription in the embryonic mouse retina (Muranishi *et al*, 2011). In 2015 Furukawa and colleagues generates tamoxifen-inducible Rax KO restricted to PRs (Rax iKO). They demonstrated that inducing Rax KO in adult PRs (1 month of age) caused a decrease in the number of S- and M- cone cells but did not influence rod number or function. Moreover, they showed that light adapted photopic (cone response) but not scotopic (rod response) ERG is significantly smaller than in control littermates (Irie *et al*, 2015). With this paper they demonstrated that in adult retina Rax has a role exclusively in cone gene expression and in maintenance of cone cells, but it is not crucial for maintenance of rod cells (Figure 15).

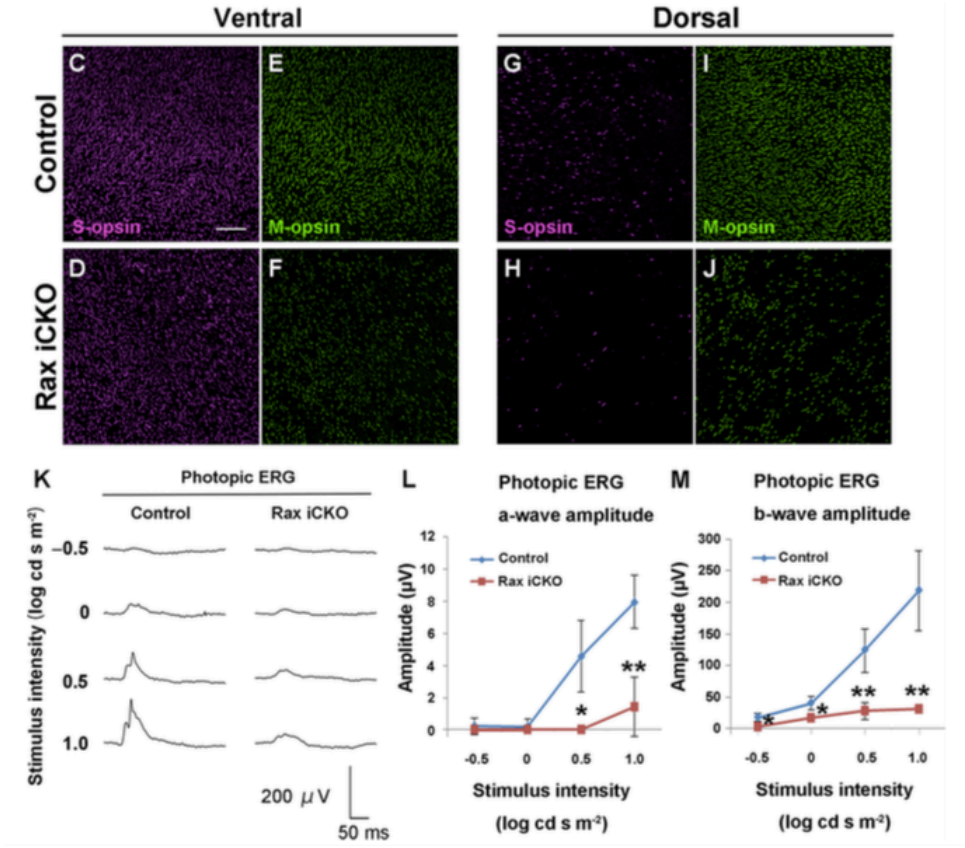

Figure 15 Rax is required for maintenance of cone photoreceptors.

(C to J) whole-mount from control and iKO Rax (induced at 1 month -> analyzed at 2 month). (K) Light adapted photopic ERG, (L and M) photopic ERG A-wave and b-wave respectively. From (Irie *et al*, 2015)

All together these reports indicate that Rax is essential both for eye development and for adult maintenance of cone homeostasis.

Chapter 3. Swine as a large animal model to study retina biology and gene therapy

3.1. Retina morphology and PR distribution in Sus scrofa

Currently, at least 90% of genetically modified pigs are generated for biomedical studies. Sequencing and annotation of the pig genome are important milestones to accelerate the generation of transgenic models. Since physiology, anatomy, pathology, genome organization, body weight, and life span of pigs and minipigs are more similar to those of humans, the domesticated pig represents an alternative biomedical model to rodents for specific human diseases.

The total photoreceptor densities in porcine retina ranged from approximately 83 000 to 200 000 cells/mm^2, with a mean of 138 500 cells/mm.

Rod:cone ratios range from 3:1 centrally to 16:1 peripherally, with a mean ratio of approximately 8:1 (Curcio *et al*, 1990), moreover the total number of cones is much more higher compared to cones number in mouse retina: 20x10^6/retina versus 180.000/retina.

3.2. Comparison between human and porcine retina

The porcine and human eye share many similarities, including a nontapetal fundus with a holangiotic vascular pattern and retinal layers of similar thickness. With the exception of the lack of a fovea, the porcine retina shares some significant similarities within the photoreceptor mosaic of humans and other primates. Primate retinas are characterized by peak foveal cone densities several times higher than peak cone densities within the pig retina (Chandler *et al*, 1999). The porcine retina has higher cone numbers compared to humans, non-human primates and mouse ($20x10^6$ compared to 4 $x10^6$, $3.1x10^6$ and $1,8x10^5$ respectively).

The enrichment in the absolute number of cones over other species makes the porcine retina very feasible to study the PR transcriptome using RNA-sequencing.

Chapter 4. Next generation sequencing methods for gene expression profiling

RNA molecules are essential component of a living cell, having a role both in gene expression and in posttranscriptional regulation. Understanding the identity and the abundance of each RNA molecule in a cell under a specific condition or in a specific genomic and epigenomic background is essentially the ultimate goal of RNA research.

High-throughput approaches are able to interrogate RNA sequences on a large scale. The first approach emerged in the early 90's. The expressed sequence tag (EST) method was developed to examine gene expression using partial sequences of cDNA clones, revealing both the sequence and the abundance of the corresponding RNAs (Adams *et al*, 1992). Many others methods were developed over the next 15 years, including the Serial analysis of gene expression (SAGE), in which only 15bp-21bp for each cDNA were sequenced (Velculescu *et al*, 1995) and DNA microarrays that superseded both EST and SAGE methods due to their much better affordability for large scale studies (Schena *et al*, 1995). The DNA microarray analysis of gene expression is based on hybridization of fluorescently labeled targets that are derived from transcript probes attached to a solid surface. The need to have sequence information *a priori* or a reference genome/transcriptome available for designing the probes limited the development and application of this technology. Indeed, next generation sequencing transformed RNA research due to its ability to acquire an unprecedented amount of data in a short time. Furthermore, compared to

DNA microarray-based methods, RNA-Seq offers less background noise and a greater dynamic range for detection. Most importantly, RNA-Seq directly reveals sequence identity, crucial for analysis of unknown genes and novel transcript isoforms.

4.1. RNA-sequencing

The power of sequencing RNA lies in the fact that the twin aspects of discovery and quantification can be combined in a single high-throughput sequencing assay called RNA-sequencing. Many variations of RNA-seq protocols and analyses have been published, making it challenging to appreciate all of the steps necessary to conduct an RNA-seq study properly. There is no optimal pipeline for the variety of different applications and analysis scenarios in which RNA-seq can be used. Hence, a RNA-seq experiment accurately designed depending on the organism being studied and the research goals is arguably the most important step for the success of the analysis (Conesa *et al*, 2016).

A general pipeline of RNA-seq preparation of a sample consists of mRNA extraction, fragmentation, ligation of adapter to distinguish forward and reverse filaments of the cDNA and barcoding of the library to have the possibility to sequence more than one sample in the same sequencing lane.

A crucial prerequisite for a successful RNA-seq study is that the data generated have the potential to answer the biological questions of interest. This is achieved by first defining a good experimental design, that is, by choosing the library type, sequencing depth and number of replicates appropriate for the

biological system under study. One important aspect of the experimental design is the RNA-extraction protocol used. Since ribosomal RNA (rRNA) represents about 90% of the total RNA in the cell, the selection of polyA RNA or the depletion or rRNA is a crucial passage to study the mRNA in the cell. Poly(A) selection typically requires a relatively high proportion of mRNA with minimal degradation as measured by RNA integrity number (RIN), which normally yields a higher overall fraction of reads falling onto known exons. Many biologically relevant samples (such as tissue biopsies) can not, however, be obtained in great enough quantity or good enough mRNA integrity to produce good poly(A) RNA-seq libraries and therefore require ribosomal depletion (Hrdlickova *et al*, 2016; Conesa *et al*, 2016).

4.2. RNA extraction and library preparation

The protocol for RNA-extraction and library preparation depends on the underlying biological question. Typically the total RNA is enriched for messenger RNA (mRNA). This can be done by either directly selecting mRNA or by selectively removing ribosomal RNA (rRNA); Poly(A) selection requires a relatively high proportion of good quality mRNA, which normally yields a high fraction of reads falling onto known exons (Wang *et al*, 2009)

Another important determinant of the quality of the sequencing is the size of the cDNA fragments obtained in this phase: a good fragmentation of the starting RNA is crucial for proper sequencing and subsequent analyses, since larger

fragments improve the mappability and de novo transcript identification. Furthermore, single-end (SE) or paired-end (PE) sequencing can be used. Although few steps are required in the preparation of an RNA-Seq sample, it does involve several manipulation stages during the production of cDNA libraries, which can complicate its use in profiling all types of transcripts.

4.3. Sequencing depth

Another important factor is the sequencing depth or library size, which is the number of sequenced reads for a given sample. More transcripts will be detected and their quantification will be more precise as the sample is sequenced to a deeper level.

4.4. Number of replicates

A crucial design factor is the number of samples required for the analysis. This depends from both the technical variability of an RNA-seq procedure and the biological variability of the system under study. These considerations are specifically relevant when designing an experiment to detect genes significantly differentially expressed between two conditions (i.e. treated samples vs. controls). It is a good standard to use at least three replicates for biological conditions, but the higher the number of replicates, the better the estimates of within-group variance, which could aspect influence the proper identification of genes differentially expressed among different conditions under study.

In general, increasing the number of replicate samples significantly improves detection of lowly expressed genes and statistical power over increased

sequencing depth (Sonia Tarazona & Fernando Garca-Alcalde, 2011).

4.5. Differential gene expression

One of the main goals of RNA-seq experiments is to identify the differentially expressed genes in two or more conditions. Such genes are selected based on a combination of expression change threshold and score cutoff, which are usually based on P values generated by statistical modeling. The expression level of each RNA unit is measured by the number of sequenced fragments that map to the transcript, which is expected to correlate directly with its abundance level.

Differential gene expression analysis of RNA-seq data generally consists of three components: normalization of counts, parameter estimation of the statistical model and testing for differential expression. Among the methods available, edgeR and DESeq/DESeq2 are the most widely used.

A common starting point for DEA methods is a count matrix N of n rows (genes) x m columns (samples) where N_{ij} is the number of reads assigned to gene i in sequencing experiment j (Rapaport *et al*, 2013).

Aims of the Thesis

Genetic differentiation programs, starting from common and genetically identical cells, control the fate of phenotypically different cell populations. The differences between these sub-populations of cells are controlled by transcriptional regulation through activation or repression of cell specific genes. In particular, during differentiation, TFs operate to control spatial and temporal expression of different developmental programs. Furthermore, after differentiation specific transcriptional factor sets confer maintenance of cell-specific identity.

The objective of this project was to investigate the transcription regulation code controlling rod-specific and cone-specific photoreceptor identity with the final aim to retrieve transcription factor sets that differentially control the gene expression of PRs. The phenotypic differences between adult rods and cones in the retina are a reflection of their different transcriptomes, which have not been characterized as yet. For this reason, the study of differential expression in PRs using next generation sequencing techniques such as RNA sequencing (RNA-seq) will provide insights into the basis for novel and relevant biological questions.

From comparative transcriptome analysis, the master regulator of retinal development Rax was found to be differentially expressed, among the others, in cone cells. To better understand the gene regulatory program of Rax, mis expression in rod cells was used as a method to identify GRN controlling cone specific phenotype. Thus assuming that a cone-specific transcription regulator

expressed in a distinct, however, to some extent similar epigenomic context, enables to retrive specific regulatory determinants of cone phenotype.

The specific aims of my Ph.D. projects have been:

i) Evaluation of Rod and Cone specific promoters

With the specific aim to characterize and compare photoreceptor transcriptomes, we characterized different rod- and cone-expressing promoters in porcine retina via sub retinal injections of AAV vectors

ii) Construction and validation of a strategy to label and select from the same retina pure populations of rod and cone

Using AAV, we exploited different strategies to obtain pure populations of rods and cones. We set up a strategy called “Double Fluo” which allowed us to isolate, after a single AAV injection, populations of rods and cones simultaneously from the same retina.

iii) RNA-sequencing and differential expression analysis of rod, cone and retina

We explored the differentially expressed genes comparing rod, cone and retina expression profiles, with the specific aim to obtain information on different TFs expressed in the two type of PRs. Furthermore, we exploited regulatory networks that underlie adult gene expression in photoreceptor cells.

iv) Rax mis-expression in rods, reveals a new role in regulation of action potential genes

We studied the role of Rax by its mis-expression in differentiated porcine rods with the specific aim to clarify which set of genes it regulates in a different epigenomic context. Thus studying somatic transcriptional control of photoreceptors may eventually result in the development of therapeutic strategies.

Materials and Methods

1. Generation of AAV vector plasmid

The plasmid used for AAV vector production was derived from pAAV2.1 plasmids that contain the inverted terminal repeats (ITRs) of AAV serotype 2 (Auricchio *et al*, 2001). AAV vector plasmids contained for either the expression cassettes the promoter, the full-length transgene CDSs and the poly-adenylation signal (pA).

The Double Fluo plasmid pAAV2.1 GRK1-mCherry-GNAT1-eGFP was generated starting from pAAV2.1 RHOΔ-ZF6-DB-GNAT1-hRHO DBR-R (S&R plasmid) (Botta *et al*, 2016).

The GRK1 promoter (Allocca *et al*, 2007; Boye *et al*, 2012; Khani *et al*, 2007) kindly provided by Professor A. Auricchio (Telethon Institute of Genetics and Medicine, Pozzuoli, Italy) was amplified from pAAV2.1 GRK1-long backbone (299bp) using primers: GRK1-nhe-fw tatatatGCTAGCgggccccagaagcctggt and GRK1-Mfe-rv tatatatCAATTGgcccttgcctgtggcccg. The PCR product was digested using NheI and MfeI restriction enzymes and subsequently cloned into pAAV2.1 S&R. mCherry was amplified from pAAV2.1 CMV-mCherry using primers: mcherry-mfe-fw tatatatCAATTGgccgccatggtgagcaagggcgagg and mcherry-Nde-rv tatatatCATATGctacttgtacagctcgtccatg. The Kozak sequence (gccgcc) was added to forward primers to have a ribosomal recognition site upstream of the CDS. The mCherry PCR fragment was digested with MfeI and

NdeI enzymes and cloned downstream of the GRK1 promoter generating pAAV2.1 GRK1-mCherry-GNAT1-hRHO-DBD-R subcloning plasmid.

The eGFP CDS was digested from pAAV2.1 CMV-eGFP (Auricchio *et al*, 2001) and cloned downstream of the GNAT1 promoter replacing the hRHO-DBD-R CDS, using NotI and HindIII restriction sites. The total length of pAAV2.1 GRK1-mCherry-GNAT1-eGFP from 5' ITR to 3'ITR was 3915 base pairs.

2. AAV production and characterization

AAV vectors were produced by the TIGEM AAV Vector Core by triple transfection of HEK293 cells followed by two rounds of $CsCl_2$ purification (Mueller *et al*, 2012). For each viral preparation, physical titres [genome copies (GC)/mL] were determined by averaging the titre measured by dot-blot analysis (Drittanti *et al*, 2000) and by PCR quantification using TaqMan (Applied Biosystems, Carlsbad, CA, USA) (Mueller *et al*, 2012). The probes used for dot-blot and PCR analyses were designed to anneal with either the ITRs or regions within 1Kb from the ITRs.

3. Subretinal injections of AAV in pig

This study was carried out in accordance with the Association for Research in Vision and Ophthalmology Statement for the Use of Animals in Ophthalmic and Vision Research and with the Italian Ministry of Health regulation for animal procedures. All procedures on mice were submitted to the Italian Ministry of

Health; Department of Public Health, Animal Health, Nutrition and Food Safety. The Ministry of Health approved the procedures by silence/consent, as per article 7 of the 116/92 Ministerial Decree. Surgery was performed under anesthesia and all efforts were made to minimize suffering.

Subretinal delivery of AAV vectors to the pig retina was performed as previously described (Mussolino *et al*, 2011). Briefly, before surgery, eyes were dilated with topical 2.5% phenylephrine (Bausch & Lomb Ltd., London, UK). The surgical procedure envisaged two-port sclerotomy, one for the light source and the other for the injection. The procedure started with a transconjunctival scleral tunnel incision via pars plana parallel to the corneoscleral limbus at 3.5 mm. The angle insertion of 20- or 23-gauge stiletto blade (Alcon, Fort Worth, TX, USA) was performed for every case to facilitate the efficiency of self-sealing. Subsequently, the light fiber attached to the vitrectomy unit (ACCURS vitrectomy machine, Alcon) and either a 38-gauge (Alcon) or extendible 41-gauge subretinal injection needles (DORC, Zuidland, the Netherlands) were, respectively, inserted through the two conjunctival incisions and into the two scleral tunnels. Therefore, illuminating the posterior pole with the light fiber and without vitreous removal, the injection in the subretinal space in the nasal area was performed with a 1-ml syringe connected to the subretinal needles, slowly and under direct observation with a stereoscopic microscope. At the end of surgery, paracentesis with removal of 0.1 ml of aqueous humor was performed using a 1-ml syringe with 30-gauge needle to collect anterior chamber fluid sample (preoperative) and to avoid an increase in intraocular pressure. All eyes

were treated with 140 μL of AAV2/8 vector solution. AAV2/8 GRK1-mCherry_hGNAT1-eGFP was injected at the dose of $1x10^{12}$ gc/eye. AAV2/8 hGNAT1-hRAX2aeGFP was injected at the dose of $5x10^{11}$ gc/eye.

All the surgery procedures were performed by the ophthalmological surgery team from the Seconda Università di Napoli (SUN).

4. Evaluation of transduction

To evaluate eGFP and mCherry expression in histological sections, eyes of Large Withe pigs (Mussolino *et al*, 2011) were enucleated fifteen days after AAV 2/8 subretinal injection. The porcine eyeball was cut at ora serrata and the humor vitreo was carefully removed. The eye was cut as flat mounts and the transduction was evaluated using fluorescence stereomicroscope and transduced and non-transduced areas were collected.

5. Histology and fluorescence microscopy

Transduced and non-transduced areas of porcine eyes were fixed in 4% paraformaldehyde overnight and infiltrated with 30% sucrose overnight; The residual humor vitreo was removed and the samples were embedded in optimal cutting temperature compound (O.C.T. matrix, Kaltek, Padua, Italy). Serial cryosections (12 μm thick) were cut along the horizontal meridian and progressively distributed on slides. The distribution of AAV2/8 GRK-1-mCherry-GNAT1-eGFP vector has been evaluated as follows: retinal cryosections n=3 eyes were analysed under a confocal fluorescent microscope (Carl Zeiss LSM

700) using either the FICT (to visualize $eGFP^+$ cells) and PE (to visualize $mCherry^+$ cells) filters.

6. Immunostaining

For cone arrestin immunofluorescence: frozen retinal sections were washed once in PBS and then fixed for 10 minute in 4% paraformaldehyde. Permeabilization solution was then added for 1hr at room temperature (0,2% Triton X-100, 1% normal goat serum in PBS 1X). Then the sections were rinsed three times for 5 minute each and blocking solution was added for 1hr at room temperature (10% normal goat serum in PBS 1X). The primary antibody, rabbit anti-human cone arrestin kindly provided by Dr. Cheryl M. Craft (Doheny Eye Institute, Los Angeles, CA) diluted 1:10000 in 10% NGS, was added overnight at 4°C. After three rinses with 0.1 M PBS, sections were incubated in goat anti-rabbit IgG conjugated with Texas red (Alexa Fluor 647, anti-rabbit 1:1000, Molecular Probes, Invitrogen, Carlsbad, CA) for 1 hr followed by three rinses with PBS. For GNAT2 immunofluorescence: frozen retinal sections were washed once in PBS and then fixed for 10 minute in 4% paraformaldehyde, after which permeabilization and blocking were made together with PBS 1X 0,3% Triton-X 20 and 5% of donkey serum for 1hr at room temperature. Sections were immunostained with primary Ab anti-GNAT2 (Santa Cruz, CA, USA) 1:200 for 2 hr at room temperature and overnight at 4°C. After three rinses with 0.1 M PBS, sections were incubated in PBS 1X 1% donkey serum with goat anti-rabbit IgG conjugated with Texas red (Alexa Fluor 594, anti-rabbit

1:500 (Molecular Probes, Invitrogen, Carlsbad, CA) for 1 hr followed by three rinses with PBS.

7. Retinal cell disaggregation

Retina disaggregation was performed following the Worthington papain dissociation kit (Worthington Biochemical, Lorne Laboratories, UK) modifying the manufacturer's protocol. In brief, all solutions were equilibrated in an incubator at 37°C and 5% CO_2 to stabilize the pH.

Transduced areas from porcine retina were collected and digested in 1ml of papain 20U/ml and 0,005% of DNAseI dissolved in HBSS solution with phenol red for 45' to 1hr in controlled temperature and CO_2 conditions (37°C and 5% CO_2). The digested samples were centrifuged at 300g for 5 minutes; the pellet was suspended in 250 μL of EBSS, albumin ovomucoid inhibitor and DNAsiI. The re-suspended cells were placed in an incubator for 15 minutes. Then, the cells were separated from cell debris using an albumin gradient (70g for 6 min at room temperature).

The single cell suspension was prepared in a FACS-optimized solution composed of PBS 1X with FBS 1%, EDTA 2mM.

8. FACS analyses and sorting

FACS analysis and sorting were carried out using a BD FACSAriaIII equipped with three lasers (488-561-647). Single cell suspensions from n=3 eyes were

stained with 15 μL of 7AAD live-dead dye (BD Bioscience, San jose, Ca, USA) to exclude dead cells from the analysis. Cells were sorted for $FITC^{+ve}/PE^{+ve}$ and $FITC^{-ve}/PE^{+ve}$. Positive cells were collected in CO_2-independent medium (Invitrogen, Waltham, MA, USA) supplied with 1% fetal bovine serum, FBS (Gibco,). FACS gates were set according to negative controls represented by untransduced retinal cells from the same eye. Gating to minimize cell doublets was applied using FSC and SSC –width. Drop delay time (ms) was calculated using Accudrop beads (BD Bioscience, San jose, Ca, USA) and the Drop 1 value was stable during all the sorting procedures.

9. RNA extraction cDNA production and qRealTime PCR

RNA was extracted immediately after the sorting of cell populations. Cells were centrifuged at 800g for 10 minute and the pellet was re-suspended in 350 μL of RLT buffer. Total RNA was extracted using the RNeasy MiniKit (Qiagen, Milan, Italy). cDNA was generated using the QuantiTect reverse transcription kit (Qiagen, Milan, Italy), 500 ng of RNA per sample was used.

PCR with cDNA was carried out in a total volume of 20 µl, using 10 µl LightCycler 480 SYBR Green I Master Mix (Roche, Basel, Switzerland) and 400 nM primers under the following conditions: pre-Incubation, 50°C for 5 min, cycling: 45 cycles of 95°C for 10 s, 60°C for 20 s and 72°C for 20 s. Each sample was analysed in duplicate in two independent experiments. Rod and cone transcript levels were measured by quantitative Real Time PCR using LightCycler 480 (Roche) using the following primers: pRho forward

ATCAACTTCCTCACGCTCTAC and pRho reverse ATGAAGAGGTCAGCCACTGCC; pGnat1 forward TGTGGAAGGACTCGGGTATC and pGnat1 reverse GTCTTGACACGTGAGCGTA; pNRL forward CAGAGCTGCTGCAGTGTCA and pNRL and reverse GTTCAACTCGCGCACAGAC; pGNAT2 forward CCATCTCAGCATTTGTTTTCC and pGNAT2 reverse GGAATGGCGAGCATTAGAAG; pOPN1Mw forward GCAGACCACCATCCATCTCT and pOPN1Mw reverse ACCTGGCAGAGACCATCATC; pOPN1Sw forward GCTCCAAGCATGCACTGATA and pOPN1Sw reverse GGGCGAGAGGGTACGATGTAG

10. RNA-sequencing library preparation, sequencing and alignment

The nine libraries (Rod, Cones and Retina), n=3 for each sample, were prepared using the TruSeq RNA v2 Kit (Illumina, San Diego, CA) according to the manufacturer's protocol. Libraries were sequenced on the Illumina HiSeq1000 platform and in 100-nt paired-end format to obtain approximately 30 million read pairs per sample. Sequence reads were trimmed using Trim Galore! software (v.0.3.3), that removes adapter sequences and trims low-quality ends using the default Phred score threshold of 20. The libraries were aligned on the full transcriptome for Sus scrofa (Pig) as provided by ENSEMBL (SusScrofa 10.2.73). The GTF included the sequences for the 20 canonical chromosomes plus 4,563 scaffolds, and counted 30.567 transcripts plus the sequences for the

2 exogenous genes used in the analysis (eGFP and mCherry). Alignment was performed with RSEM (v.1.2.11) with default parameters. The resulting expected counts (the sum of the posterior probability of each read coming from a specific transcript over all reads) were used for subsequent analysis. All the bioinformatics procedures were performed with the help of the TIGEM Bioinformatics core.

11. DAVID Gene ontology analysis

Gene ontology analyses were performed using the Functional Annotation tool of DAVID 6.8®. GO classes were selected using an FDR threshold of 5%. All the analyses were performed using *Homo sapiens* GO background.

12. STRING analysis

Protein-Protein interaction analyses were performed using the STRING database.

13. Elettroretinogram recordings

Bilateral full-field ERGs were recorded by a computer-based system (EREV 2000) and corneal contact lens electrodes with a Ganzfield stimulator according to the ISCEV protocol (Marmor *et al*, 2004). Elena Marrocco, from Enrico Maria Surace's group, performed Elettroretinogram analyses.

Results

1. Evaluation of Rod and Cone specific promoters

To isolate cone and rod populations, we took advantage of the characteristics of the porcine retina, including the size and photoreceptor composition since the porcine retina possesses a higher number of cones compared to mouse and NHP.

Rod specific promoter comparison was performed using the modified version of the human Guanine Nucleotide Binding Protein Alpha Transducing (GNAT1) promoter published in the Corbo lab in 2010 (Lee *et al*, 2010) and the first 800 base pairs (bp) of the human rhodopsin (RHO) promoter**.** Efficacy of hGNAT1 promoter compared to hRHO proximal promoter was evaluated in vivo.

AAV 2/8 expressing eGFP driven by hGNAT1 was injected into the sub retinal space of adult porcine retina, injecting the same expression cassette driven by hRHO promoter at the dose of $1x10^{10}$ genome copies (GC)/eye. Fifteen days after sub retinal injection, both the spatial distribution and the level of expression using histological sections were evaluated. Histological sections showed a comparable expression level between hGNAT1 and hRHO promoters; however, eGFP expression showed an apparent wider distribution in hGNAT1-treated retinae than in hRHO (Figure 16).

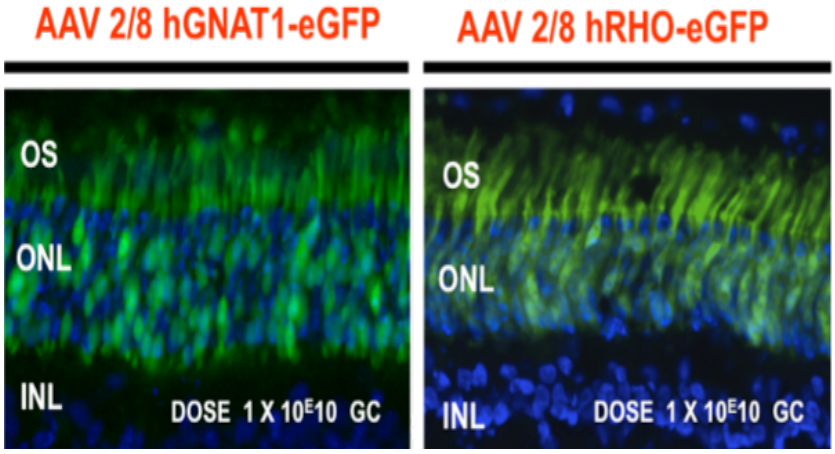

Figure 16 Comparison of hGNAT1 and hRHO promoters.

Fluorescence analysis on cryosection from porcine retina fifteen days after a single subretinal injections of AAV2/8 encoding for eGFP under the control of human rhodopsin hRHO or human Guanine Nucleotide Binding Protein alfa transducine hGNAT1, in the contralateral eye. OS: outer segment, ONL: Outer nuclear layer, INL: inner nuclear layer. In blue DAPI: 4',6'-diamidino-2-phenylindole staining; EGFP: native EGFP fluorescence. Dose $1x10^{10}$, n=3.

One of the main limitations encountered in retinal gene transfer (using *Sus scrofa* retina to study photoreceptors) is the scarcity of promoter elements enabling cone specific expression. In 2014 Hauswirth's group published a study that described and compared the efficiency of different promoters for the specific expression of transgenes in murine cone photoreceptors (Dyka *et al*, 2014). They demonstrated that a combination of the enhancer of interphotoreceptor retinoid-binding protein (IRBP) and the proximal promoter region of the cone alpha transducine (GNAT2) was able to specifically transduce mouse cones. To test the effectiveness in transducing porcine cone cells,

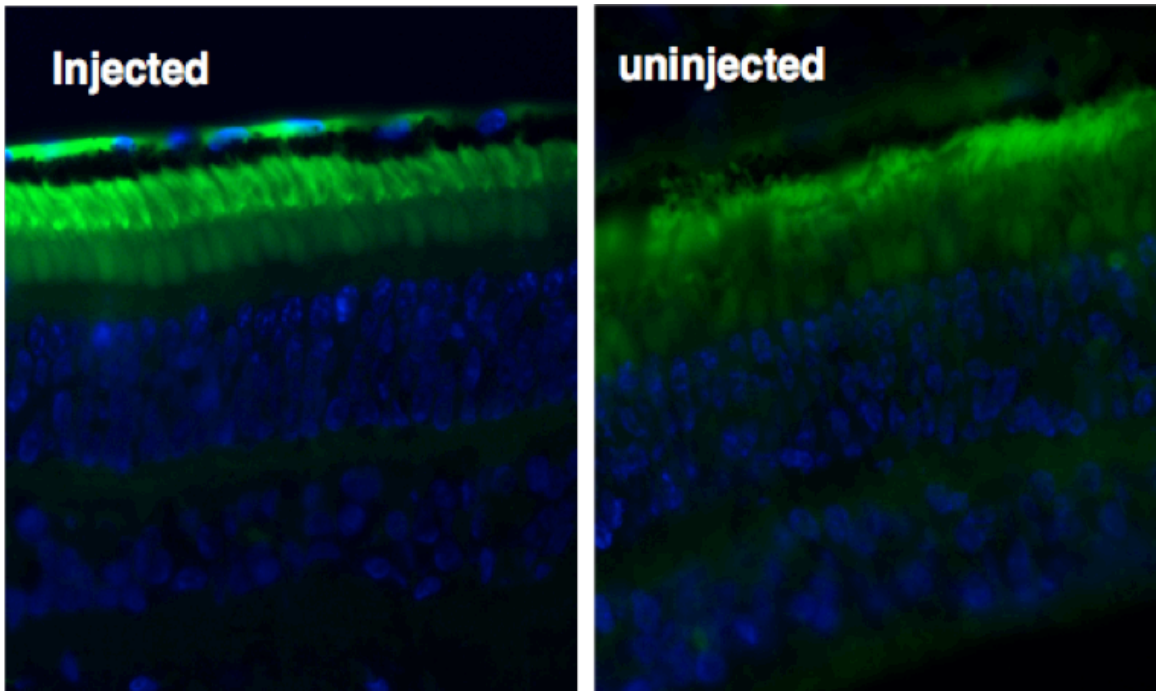

Figure 17 Subretinal injection of AAV2/8 eIRBP-hGNAT2-eGFP

Fluorescence analysis on cryosection from porcine retina fifteen days after a single subretinal injections of AAV2/8 encoding for eGFP under the control of a chimeric regulative element composed by human enhancer of Interphotoreceptor Retinoid-Binding Protein (eIRBP) and human Guanine Nucleotide Binding Protein alfa transducin 2 hGNAT2 promoter. PBS injected contralateral eye as negative control. In blue DAPI: 4',6'-diamidino-2-phenylindole staining; EGFP: native EGFP fluorescence. Dose $1x10^{10}$, n=3.

the IRBP-GNAT2 promoter was cloned into the pAAV 2.1-based backbone and injected via AAV8 in three independent porcine retinae at the dose of $1x10^{12}$ GC per eye. Fifteen days after injection, the animals were sacrificed to evaluate eGFP expression compared to uninjected contralateral eye. Immunofluorescence analysis showed no differences between injected and control (Figure 17), suggesting that despite a good efficiency in mouse retina this chimeric promoter was not able to drive the gene expression in porcine cones.

To overcame the lack of cone-specific promoter elements for the porcine retina, a different strategy to lable cones was evaluated. Several papers demonstrated

the high and specific gene expression in both rod and cone PRs of the human rhodopsin kinase promoter (hRHOK), also known as G Protein-Coupled Receptor Kinase 1(GRK1), both in mouse and in non human primates retina (Boye *et al*, 2012; Khani *et al*, 2007; Young *et al*, 2003).

Based on this obervation a strategy that combined the use of both hGRK1 and hGNAT1 promoters was tested creating a recombinant AAV genome (rAAV) containing two independent expression cassettes: hGRK1-mCherry and hGNAT1-eGFP genes (Figure 18A).

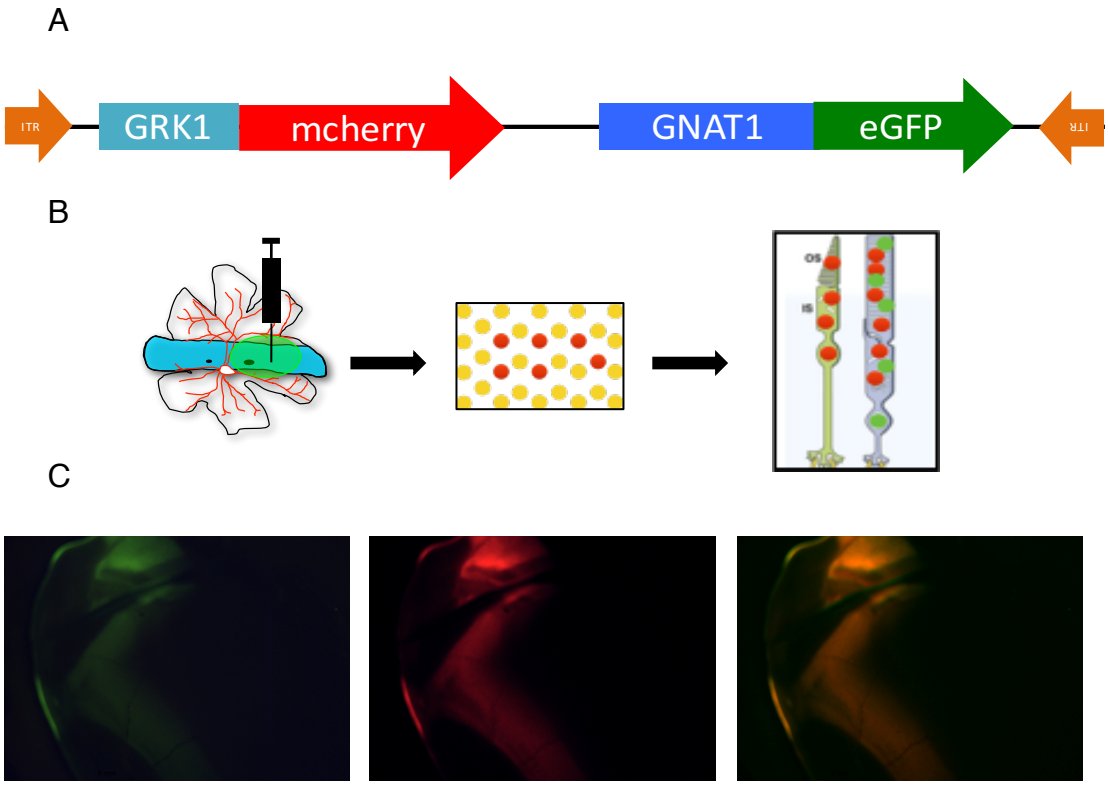

Figure 18 Double Fluo strategy to transduce simultaneously rod and cone in porcine retina

(A) Schematic representation of "Double fluo" AAV 2 genome and injection strategy (B). mCherry coding sequence (CDS) under the control of G protein coupled receptor kinase 1 (GRK1) promoter is coupled with eGFP CDS controlled by Guanine Nucleotide Binding Protein alfa transducin 1 promoter (GNAT1). Fluorescence stereomicroscopy of representative retina, fifteen days after double fluo AAV 2/8 subretinal injection. native eGFP (left panel), mCherry (central panel), merge (right panel). Dose: $1x10^{12}$ GC.

Thus, we hypothtized that the expression of the mCherry marker (red) gene expressed in both rods and cones combined with the exclusive expression of eGFP (green) in rods would enable the differential labeling of rods (double fluorescence red and green: yellow signal) and cones (single fluorescence: red signal).

Three independent subretinal injections were performed with the “double fluo” AAV vector at the dose of $1x10^{12}$. Animals were sacrificed fifteen days post injection evaluating the double transduction and sampling using a fluorescence stereomicroscope (Figure 18 B and C).

The histological sections of “Double Fluo vector” treated eyes showed strong colocalization between eGFP and mCherry in rod cells and the presence of the mCherry signal characterizing cones (Figure 19 A)

To confirm mCherry expression only in cones and to exclude any possible leakage between rod and cone signals, arrestin 3 (Arr3) immunofluorescence was performed. Arr3, also known as cone arrestin (CAR), is one of the cone’s phototransduction proteins, distrubuted along the entire cone soma. Its localization makes it especially useful to confirm our strategy. Immunofluorescence showed co-localization between CAR and the endogenous mCherry fluorescence and absence of colocalization between the CAR signal and eGFP/mCherry labled rods (Figure 19 B and 20 A).

Furthermore to exclude any possible toxicity due to the high AAV dose injected, retinal thickness, rhodopsin (RHO) localization and Iba1 positive microglia infilration, in outer nuclear layer (ONL), were evaluated. The analyses showed

normal morphology of the “Double Fluo” treated retinae and both proper RHO localization and absence of microglia cells in the ONL (Figure 21 A and B)

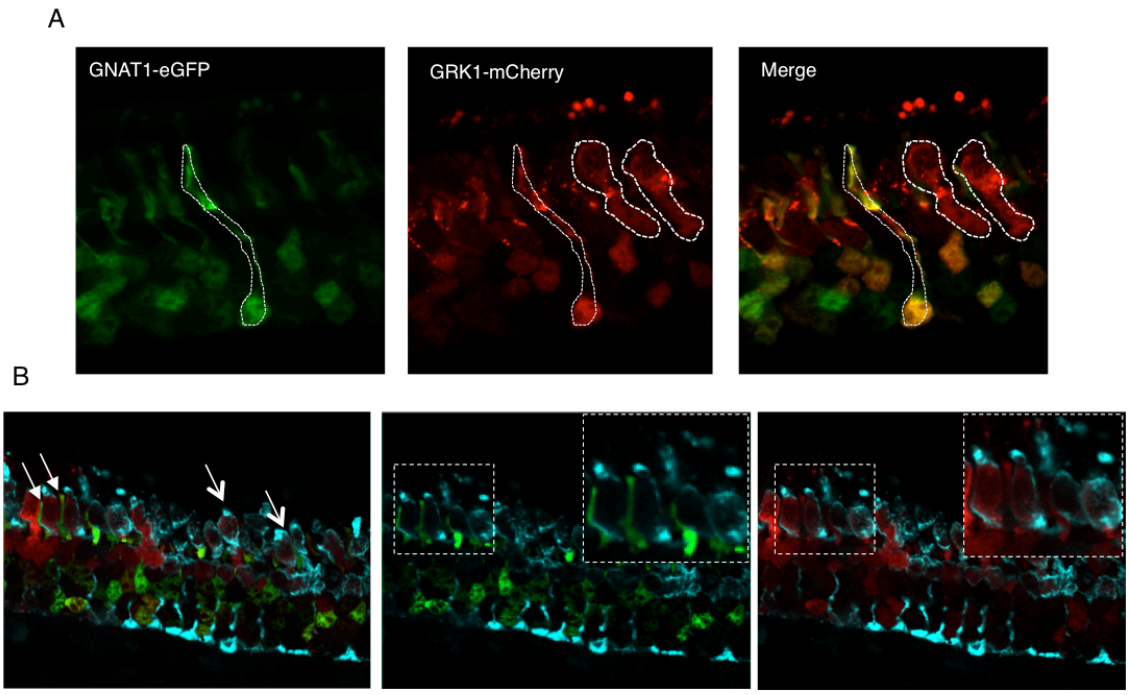

Figure 19 AAV 2/8 hGRK1-mCherry-hGNAT1-eGFP transduction in porcine retina

Fluorescence analysis of representative porcine retinal cryosections fifteen days after injection of AAV2/8 (A) Double fluo eGFP expression in rod cells (A, left panel), mCherry signal in both rod and cone (A, central panel), merge right panel A. Arrestin 3 (ARR3) immunofluorescence (cyano) (B) Co-labeling with native eGFP and mCherry signals. Left panel, full arrows indicate rod eGFP positive, arrowheads indicate co-localization of mCherry and ARR3.

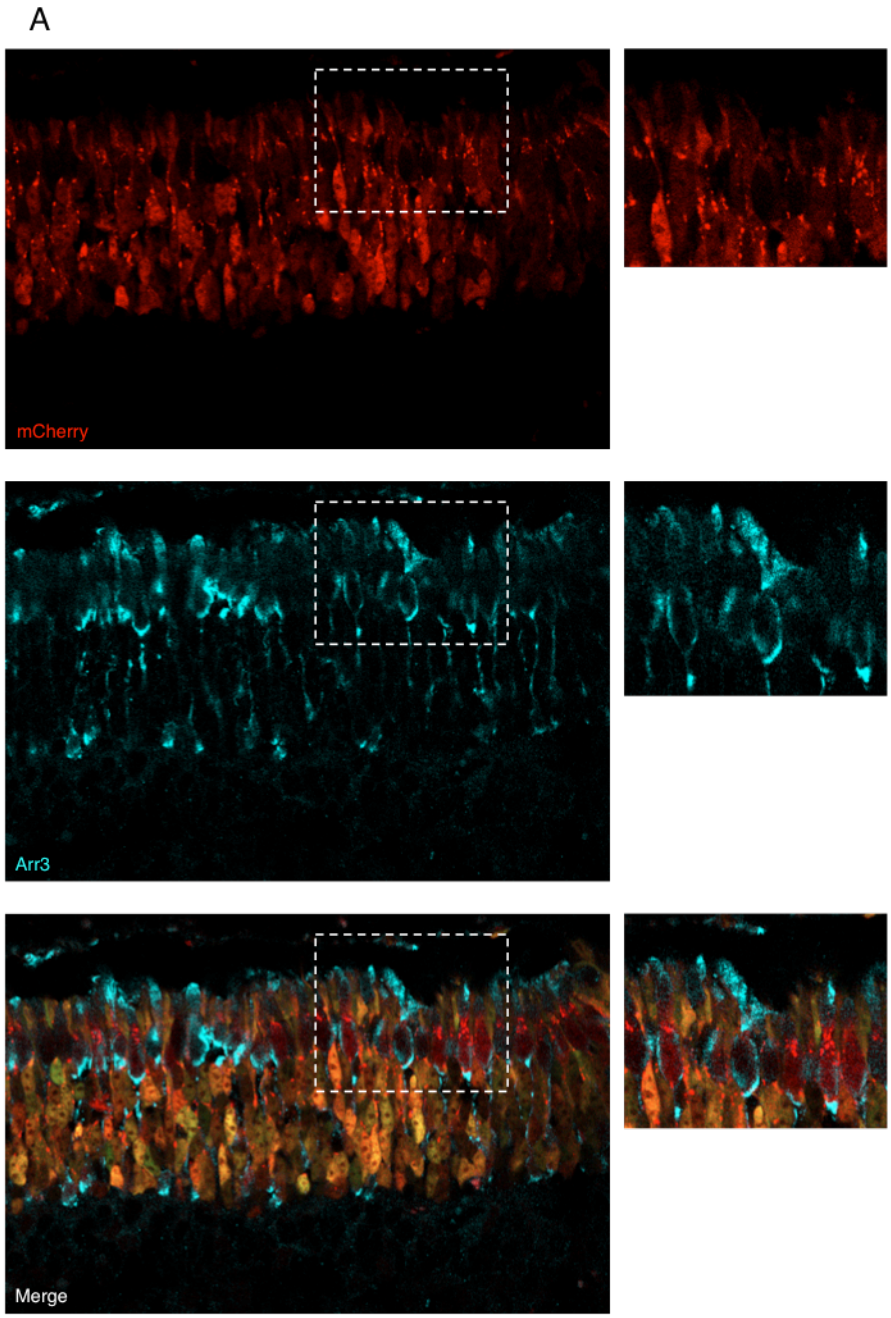

Figure 20 AAV 2/8 hGRK1-mCherry-hGNAT1-eGFP co-localization with Arr3

Arr3 immunofluorescence of "Dual Fluo" transduced porcine retina. mCherry transduction fiftheen days after subretinal injection (Upper panel). Arr3 labeling (Mid panel) and merge od mCherry signals and Arr3 (Lower panel), detail of mcherry and Arr3 co-localization in zoom.

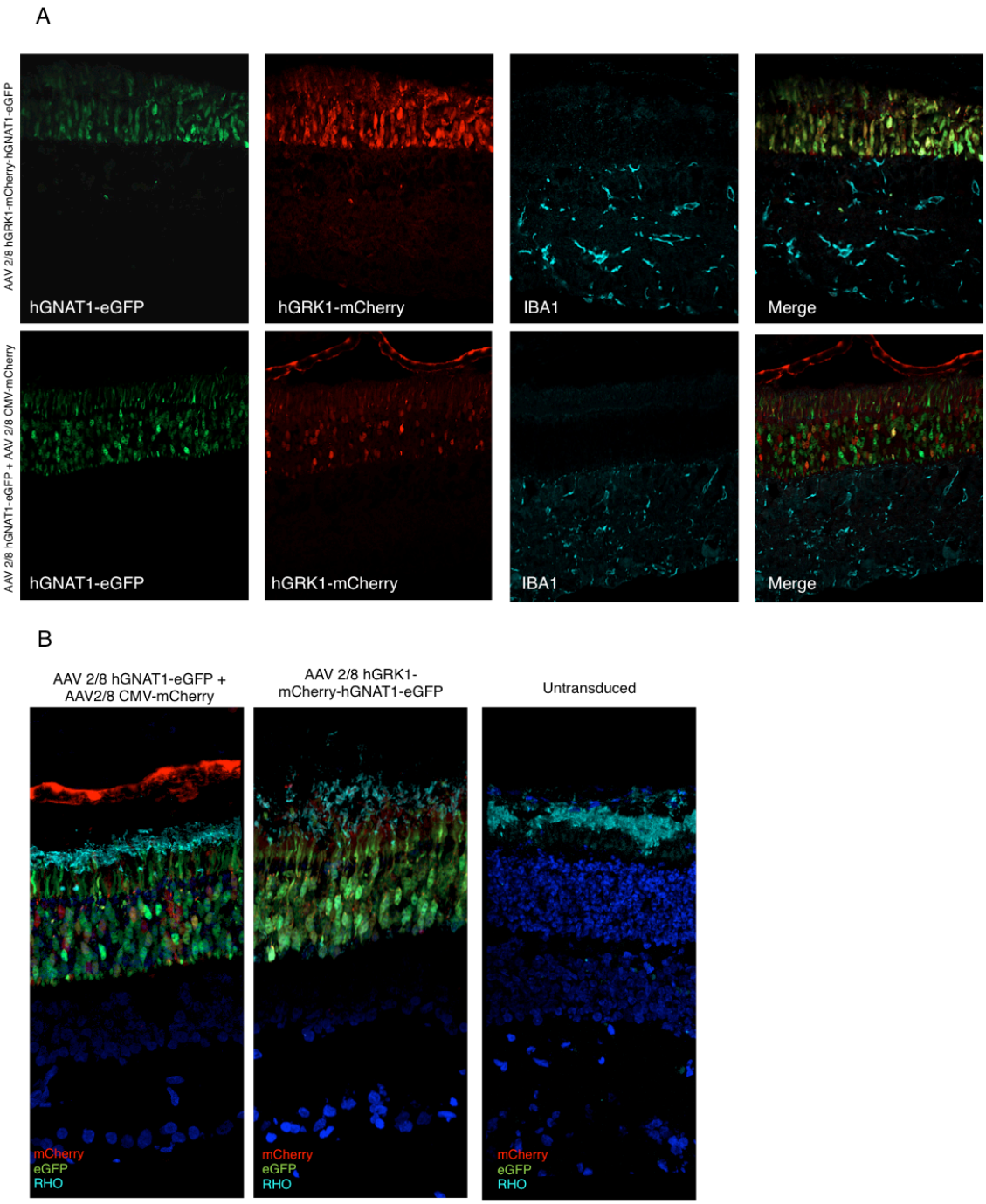

Figure 21 Microglial localization and rhodopsin evaluation in Double Fluo treated retinae

(A) Evaluation of microglial cells localization into retinae treated with Double Fluo and AAV2/8 hGNAT1-eGFP + AAV2/8 CMV-mCherry, respectively upper and lower panel. (B) Evaluation of proper rhodopsin localization into outer segment (OS) of rods.

These results demonstrated the effectiveness of the “Double Fluo” strategy to label both photoreceptors after a single AAV subretinal injection in porcine

retina. Moreover, we demonstrated the specificity of expression using two different cassettes, with two different promoters, in a single AAV genome.

2. Construction and validation of a strategy to mark and sort pure populations of rods and cones from the same retina

To further confirm the usefulness of the “Double Fluo” strategy to obtain pure populations of rods and cones, Fluorescence Activated Cell Sorting (FACS) was perfromed on “Double Fluo AAV” injected retine (N=3). The FACS analysis showed that 35% of total events (3,500 events out of 10,000 total read events), were positive for both FITC and PE, respectively eGFP and mCherry. The analysis showed 6.1% of events were only positive for the PE signal (Figure 21 A). Analysing the average of three independent experiments a ratio between rods (eGFP/mCherry-expressing population) and cones (mCherry-expressing population) of 7.6:1 was found: this ratio was similar to the physiological ratio of 8 rods for 1 cone found in the cone-rich region in which the injections were carried out (Figure 21 B).

Both fluorescent populations were selected using FACS and rod and cone specific markers analyzed. The analysis on the eGFP/mCherry-expressing population showed the specific expression of rod markers such as Rho, Gnat1 and Nrl, showing a complete absence of these markers in mCherry-expressing cells. On the other hand, qReal time PCR showed the enrichment of cone markers in the mCherry-expressing population (Figure 21 C)

Some expression of Rho and Gnat1 but not of NRL in the mCherry population was found, although this leakage was not statistically significant.

These reults demonstrated the feasibility of our system in order to obtain pure populations of live rods and cones. Moreover, the results showed that there

wasn't any cross contamination between the two populations, preserving a physiological ratio between rods and cones.

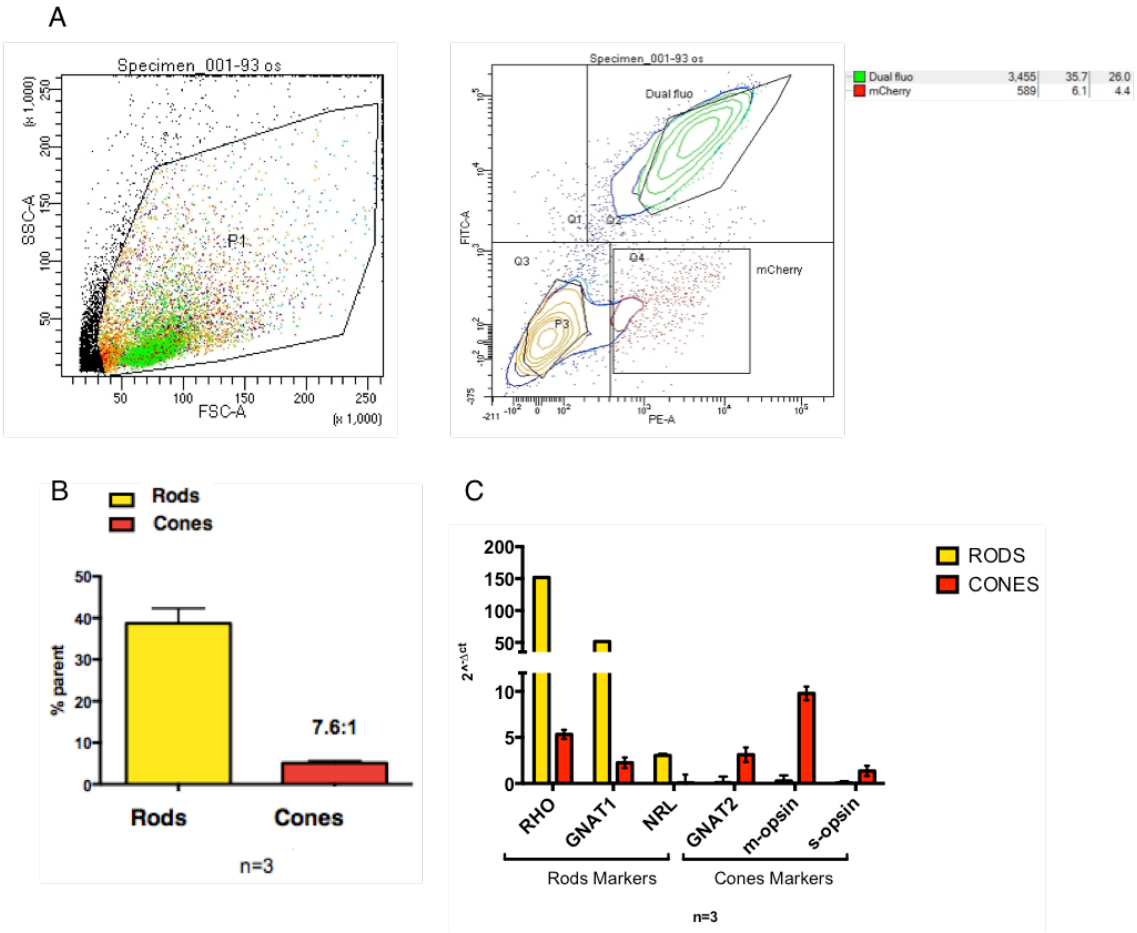

Figure 22 Double fluo selected pure population showed specific expression of rod and cone genes.

(A) Representative plots of Fluorescent Activated Cell Sorting (FACS) analysis of AAV2/8 Double Fluo transduced retinal cells. Left panel shows morphological dot plot of forward scatter area, FSC-A (x-axis) versus side scatter area (SSC-A) (y-axis), n=3. P1 gate contains observed population. Right panel shows fluorescence dot plot of fluorescein isothiocyanate, FITC (y-axis), Phycoerythrin, PE (x-axis). Double fluo and mcherry gates contain FITC-PE positive and PE positive cells respectively. Legend contains percentage of fluorescent events in each gate. (B) Left panel shows ratio between percent of FITC-PE positive cells (presumptive rods) versus PE positive cells (presumptive cones). In panel (C) the expression levels, of rod and cone genes in sorted populations. FITC-PE versus PE positive sorted cells. Mean of n=3 independent experiments.

3. RNA Sequencing of rods, cones and retina

Principal component analysis (PCA) showed a high correlation between the three biological replicates in each group. Furthermore, PCA showed a separation between Rod and Retina clusters on the dimension 1 indicating a high level of differences between these two samples. By contrast, rod and cone clusters were less separated, indicating similarities in gene expression profiles (Figure 21 A)

Differential expression analysis correlates gene expression levels in two or more different biological samples or conditions.

To study the expression profile and the DEGs between rods and cones, sequencing of total mRNA of two FACS-sorted populations was performed. To obtain more stringent analysis of differentially expressed genes from the same biological samples DEA was performed between retina, rods and cones. From these three independent DEA: Cone versus Retina, Rod versus Retina and Rod versus Cone, we focused on the intersection which identifies rod and cone exclusively expressed genes (Figure 21 B). We found 982 common genes with a significant false discovery rate (FDR) less than or equal to 0.05.

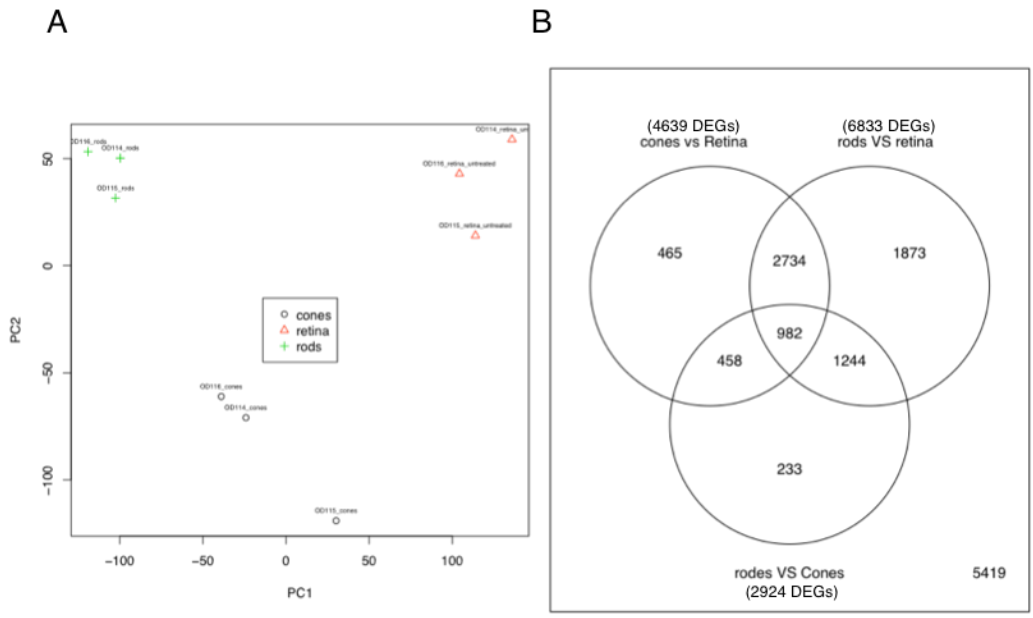

Figure 21 Differential expression analysis

(A) Principal component analysis (PCA) showing differences between three analyzed sample (B) Venn diagram of three differential expression analysis (DEA), shows 982 common genes.

Out of 982 common DEGs, applying logFC and sorting for up and down regulated genes, a total of 358 differentially expressed genes were obtained, of which 68 genes had rod-specific expression: downregulated in ConesVsRetina and upregulated in both RodVsRetina and RodVsCone. Twohundredninty genes had cone-specific expression: upregulated in ConeVsRetina and downregulated in both RodVsRetina and RodVsCone (Table 1).

Ensemble Gene Id	Gene name	logFC ConeVsRetina	logFC RodVsRetina	logFC RodVsCone
ENSSSCG00000011590	Rho	-2,53	0,92	3,45
ENSSSCG00000002010	Nrl	-1,92	1,36	3,29
ENSSSCG00000024609	Gnat1	-1,99	1,53	3,52
ENSSSCG00000002811	Cngb1	-0,92	1,96	2,88
ENSSSCG00000016580	Opn1sw	1,65	-5,78	-7,43
ENSSSCG00000029523	Opn1mw	2,95	-5,26	-8,22
ENSSSCG00000006823	Gnat2	4,07	-4,32	-8,39
ENSSSCG00000006134	Cngb3	4,04	-4,17	-8,22

Table 1 **Differential expression criteria**

In green rod genes; in red cone genes.

Approximately 4 times more DEGs were observed in cones compared to rods. Gene ontology (GO) analysis on 290 cone DE genes showed the presence of both biological processes (BP) related to visual function and to immune system activation. These results partially explain the greater number of DEGs in cones compared to the rod data set in which GO classes related to immunity were not observed (Figure 22).

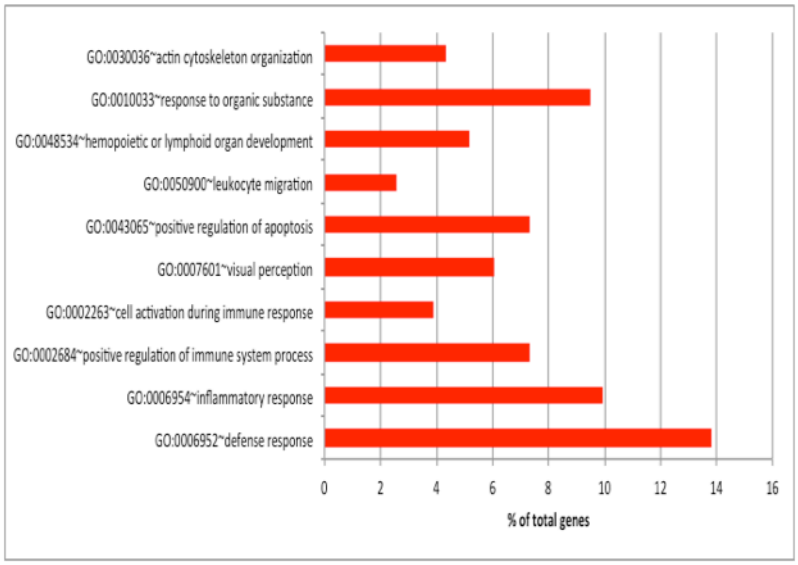

Figure 22 Gene ontology analysis of cone DEGs

Cone DEGs genes grouped in biological processes categories shows enrichment in both immune related functions and in visual perception processes.

4. Porcine correlation network (SusNet) to discriminate cone and rod co-expressed genes

Of presumptive molecular contamination of the cone dataset, network biology and community clustering were applied to obtain information about cone gene expression to try to discern cone-specific genes from immune related "contaminant genes". Analysis was performed using a porcine co-expression network built in our laboratory, called SusNet (unpublished data). Calculating the co-expression levels of 290 genes, two main genes communities were found (Figure 23 A).

The clusters were connected by six genes and the number of connections into the red cluster were higher than green. Immune related genes (such as *AIF1*, also know as *IBA1*) were found in the red cluster while cone-specific markers such as *OPN1SW*, *OPN1MW* and *THRB* were found in the green cluster.

GO analysis on genes present in the red cluster showed the absence of visual and neuronal-related biological processes and the presece of biological processes related to immunity such as response to wounding, defense response and immune effector process. Conversely, none of the classes related to immunity were found in the GO of green cluster genes (Figure 23 B-C).

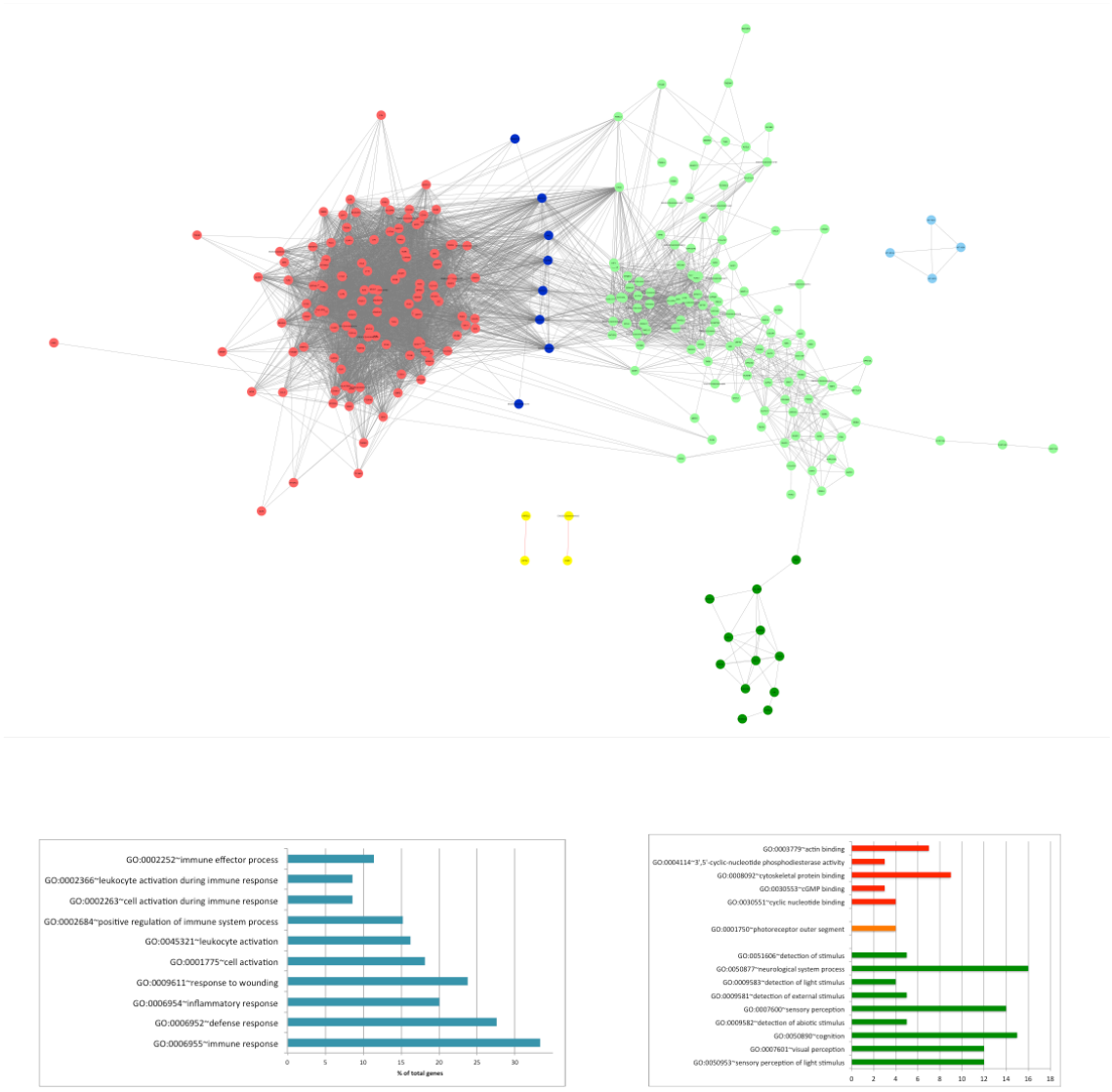

Figure 23 Gene community network of cone DEGs genes

(A) SusNet correlation analysis on 290 cone DEGs, network shows clustering of cone DEGs based on co-expression data from SusNet. (B) GO analysis of the red cluster shows enrichment in biological processes related with immune response, in (C) gene ontology analyses of 128 genes in green (light and dark) clusters showing classes related to visual functions and neurological processes.

Finally, three clusters were found applying SusNet analysis on 68-rod genes. GO analysis showed visual-related top-scored classes (Figure 24 A-B).

A

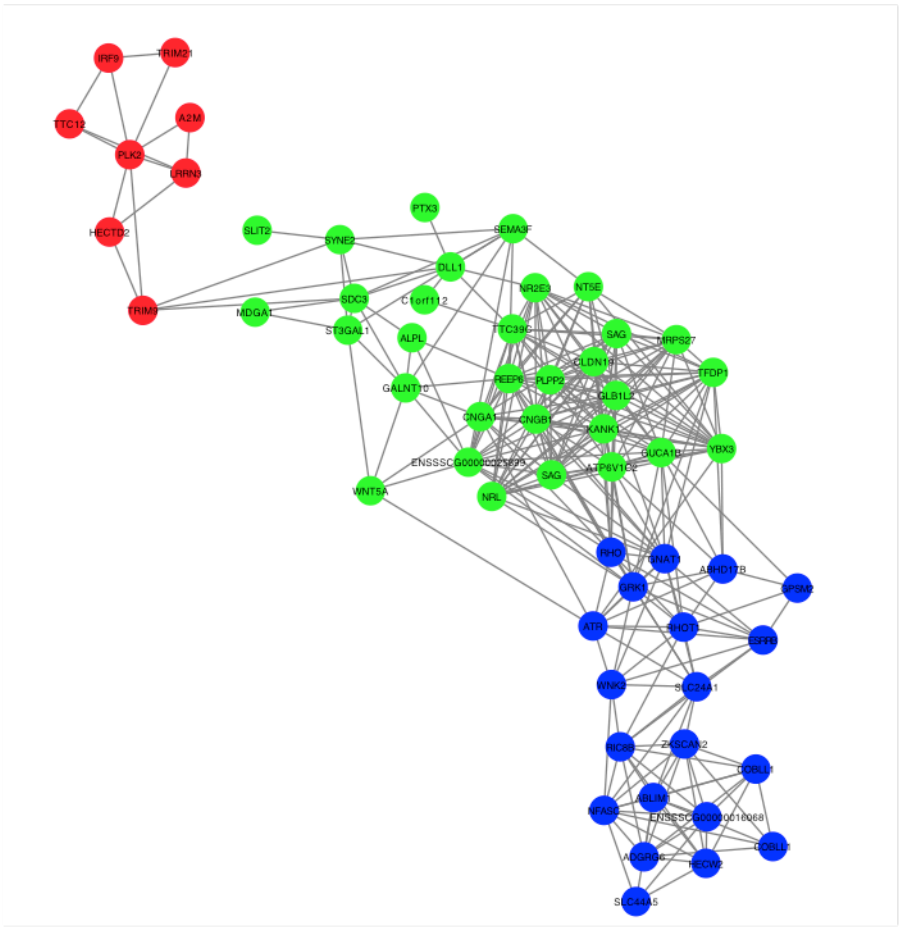

B

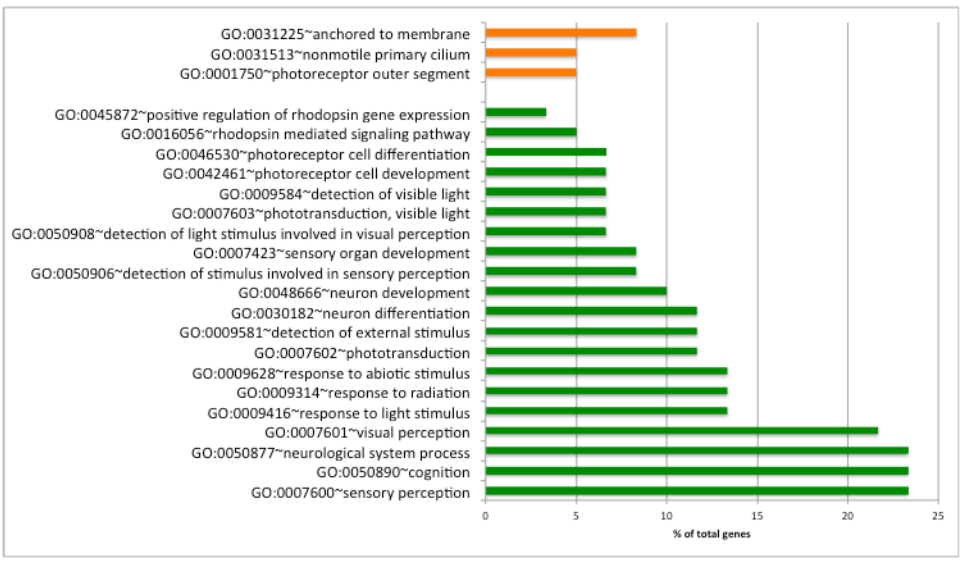

Figure 24 Gene community network of rod DEGs genes

(A) SusNet correlation analysis on 68 DEGs genes, network shows three distinct cluster of genes. (B) Gene ontology analysis on rod genes reveals GO classes associated with visual functions.

5. Analysis of differentially expressed transcription factors in Rods and Cones

Many aspects of cell differences between tissues or in the same tissue are strictly related to differential gene expression. Gene expression is regulated by diverse factors including epigenetic, histone posttranslational modifications and TFs. Transcription factors have a fundamental role forming a gene regulatory network in which a hierarchy of events terminates with a fine-tuning of gene expression.

Analyzing genes differentially expressed in rod versus cone transcriptomes and filtering the genes using GO categories, 8 transcription factors exclusively expressed in rods and 8 in cones were found (Table 2).

As expected, some well-known TFs were expressed in both photoreceptorial datasets. NRL and the nuclear orphan receptor NR2E3 were found highly and specifically expressed in rods, while TFs which expression was known to be cone specific such as Thyroid Hormone Receptor beta (THRb) were found expressed in the cone dataset.

Furthermore, other TFs previously uncharacterized in the retina were found (Table 2).

Known Described only Unknown

Ensembl ID	Gene name	Cell type	Reference
ENSSSCG00000004978	NR2E3	Rod	Cheng et al, 2011
ENSSSCG00000002388	ESRRB	Rod	Akishi et al, 2010
ENSSSCG00000002010	NRL	Rod	Swaroop et al, 1992
ENSSSCG00000009560	TFDP1	Rod	Dyer et al 2001
ENSSSCG00000014780	TRIM21	Rod	
ENSSSCG00000000633	YBX3	Rod	
ENSSSCG00000002002	IRF9	Rod	
ENSSSCG00000007823	ZKSCAN2	Rod	
ENSSSCG00000011211	THRB	Cone	Ng et al, 2001
ENSSSCG00000004910	RAX	Cone	Furukawa et al, 1997
ENSSSCG00000004858	SALL3	Cone	de Melo et al, 2011
ENSSSCG00000005086	SIX6	Cone	Carl et al, 2002
ENSSSCG00000015536	LHX4	Cone	Balasubramanian et al 2014
ENSSSCG00000012068	ETS2	Cone	
ENSSSCG00000023045	BAHCC1	Cone	
ENSSSCG00000024480	SFMBT2	Cone	

Table 2 Transcription factors expressed in rods and cones.

(Cheng *et al*, 2004; Omori *et al*, 2011; Aguilar *et al*, 2016; Carl *et al*, 2002; Dyer & Cepko, 2001; Swaroop *et al*, 1992)

Binding analysis, aimed to predict the hierarchy between these factors, was performed. Using position weight matrix of differentially expressed TFs we carried out prediction of binding on the promoter sequences (-2000bp;+200bp) of these transcription factors (Figure 25).

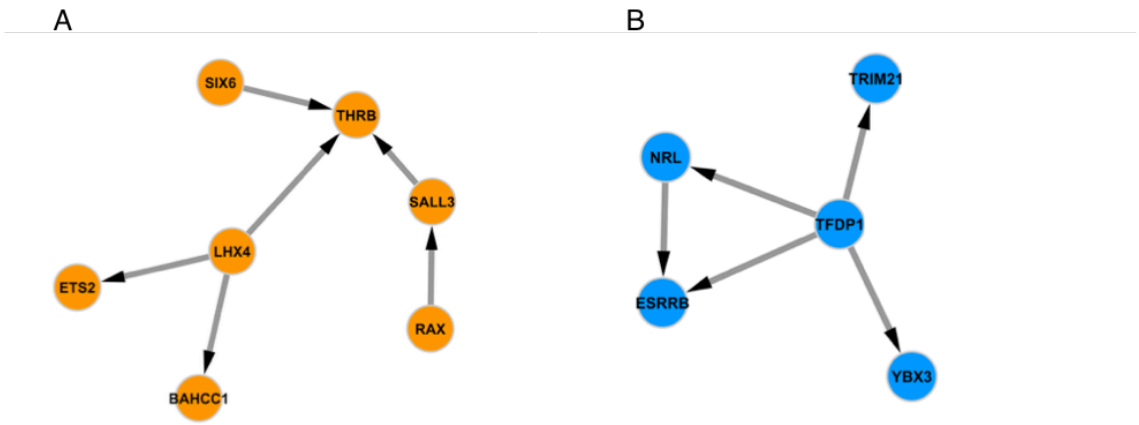

Figure 25 Binding predictions of differentially expressed transcription factors

Transcription factors prediction of binding in rod (A) and cone (B). Direction of arrows indicates the binding of TF on a promoter element. Analyses were performed using Transfac Match tool on porcine promoter sequences from -2000 to +200 bp relative to TSS.

Binding analysis showed a putative regulatory axis between RAX, SALL3 and THRB in cones, whereas the transcription factor DP1 (TFDP1) seemed to have a central role in binding and possibly regulate rod-specific TFs, including NRL and Estrogen Related Receptor Beta (ESRRB).

In silico gene regulatory network (GNR) analysis was performed by Transfac, predicting binding of DE TFs from rods and cones on promoter sequences of DEGs belonging into the categories of common genes between the three DEAs. (Figure 26)

The rod GRN showed NRL and TFDP1 as central TFs in binding rod-only expressed genes while cone-binding prediction showed a number of TFs involved in a GRN that was higher than in rods. RAX, SALL3 and SIX6 showed a sub-network both controlling common targets and binding each other.

This analysis showed a possibly role of TFDP1 in the regulation of different photoreceptorial genes in combination with NRL and a putative role of TFs

generally expressed in mouse developing retina such as RAX, SIX6 and SALL3 in porcine adult cones (Figure 26).

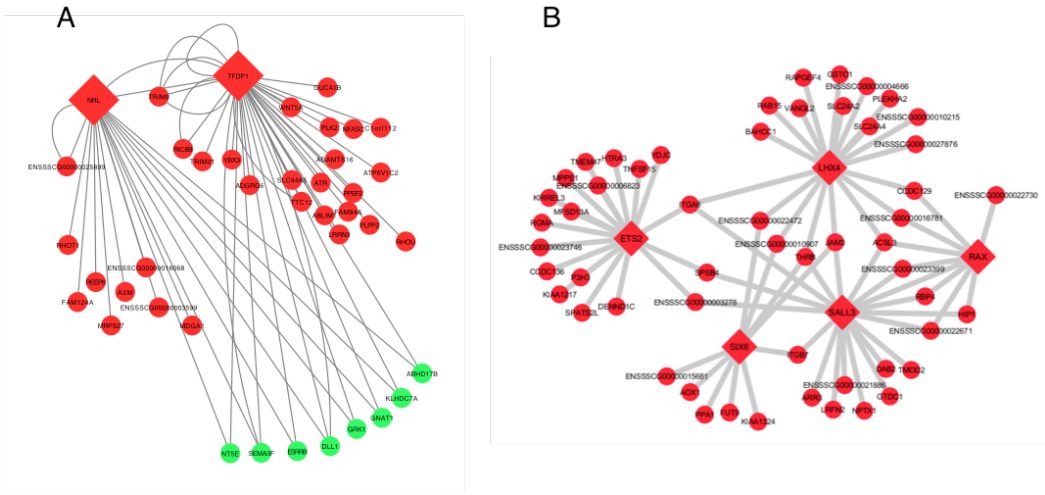

Figure 26 In silico reconstruction of Rod and Cone gene regulatory network

(A) Transfac binding prediction showed NRL and TFDP1 (red diamonds) connected to 35 out 68 rod DEGs. Common genes are indicated in green circle. (B) TFs binding prediction in cone DEGs showed a network 58 out of 128 differentially expressed genes. TFs indicated as diamonds.

Further studies are required to demonstrate and validate the binding prediction that showed new TFs involved in rod and cone gene regulatory networks.

6. RAX overexpression in rods reveals a new role in regulation of action potential genes

Retina And Anterior Neural Fold Homeobox was one of the TFs found in the differential expression analysis of rods versus cones. In particular, *Rax* expression was down regulated in rods vs cones, resulting in 10^2 times more expressed in cones than in rods (Figure 27).

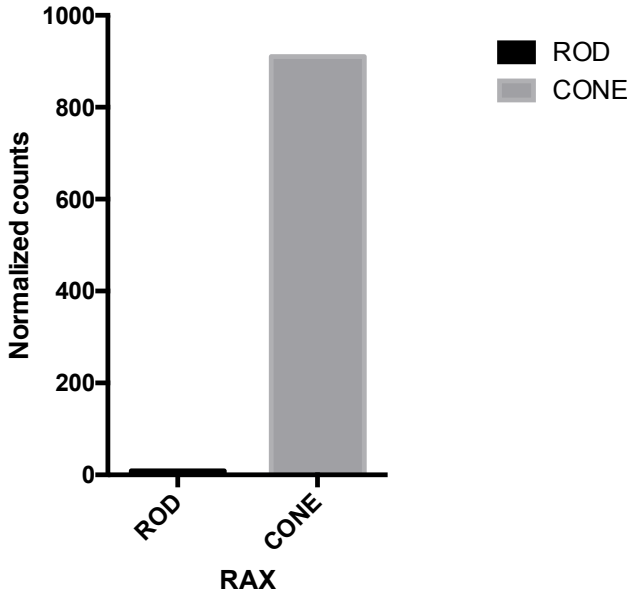

Figure 27 Rax gene expression level in rod and cone

Rax normalized counts from RNA-sequencing comparing Rod versus Cone expression dataset. Fold change: ~100 cone/rod.

In addition, i) Rax was found upstream in the predicted binding network (Figure 26A) among retrieved cone-specific TFs; ii) Rax is critically involved in murine retinal development, and iii) in maintenance of post-mitotic murine cones (Muranishi *et al*, 2011; Furukawa *et al*, 1997a; Irie *et al*, 2015). Thus, based on these criteria Rax was selected to study its cone regulatory role in post-mitotic cones. Towards this objective we sought to investigate whether Rax ectopic

expression in rods, which possess a similar, however, distinct epigenomic background, enables to extract its cone specific GRN. AAV 2/8 containing the human RAX CDS 2A eGFP driven by the hGNAT1 promoter was subretinally injected into adult porcine retinae and the contralateral eye was injected with AAV2/8 hGNAT1-eGFP as a control at the same dose ($1x10^{11}$ viral particles/eye). eGFP-positive rods were selected by FACS (Figure 28) and total mRNA was used for deep sequencing.

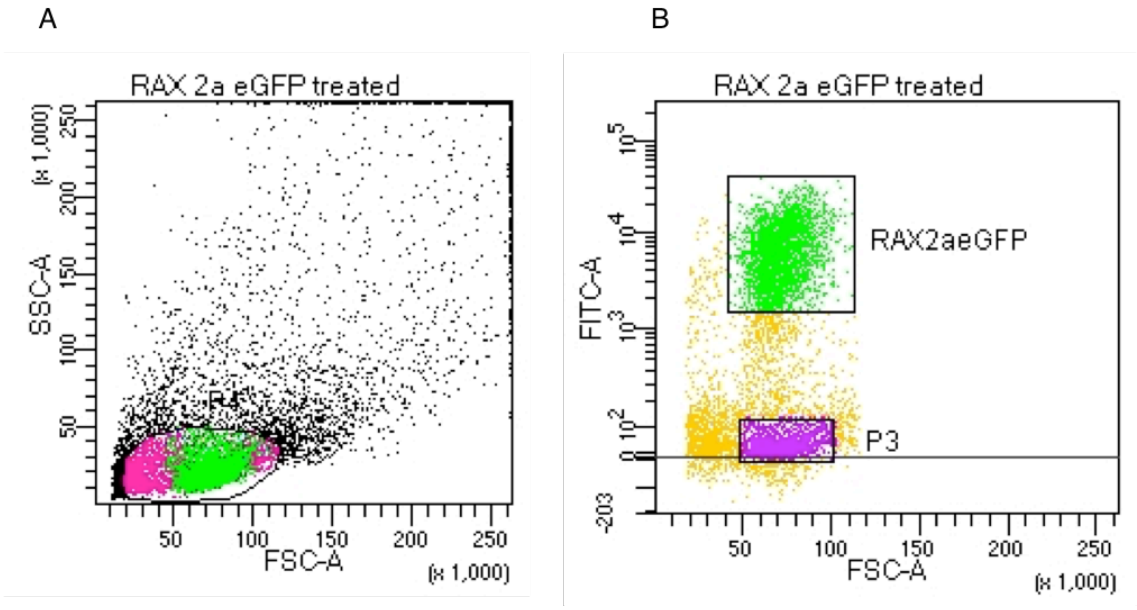

Figure 28 RAX treated rods selection via FACS

(A) Morphological dot plot of side scatter area, SSC-A versus forward scatter area,FCS-A, P1 indicate population of interest. (B) Fluorecence (FITC-A) versus FSC-A, RAX2aeGFP indicate rod treated, selected for cell sorting.

RNA sequencing showed a total of 386 DEGs out of which 224 genes (58%) were up- and 162 (42%) down-regulated (FDR 0,05 and logFC 1,5). DAVID GO analysis on up-regulated genes showed a significant enrichment of biological processes associated with ion and transmembrane transport; in particular action potential was the most significant classes based on false discovery rate (FDR)

resulting in 7 up regulated genes (*HCN2, KCND2, SCN3B, NALCN, KCNIP2, CXADR, KCNJ3*) (Figure 29).

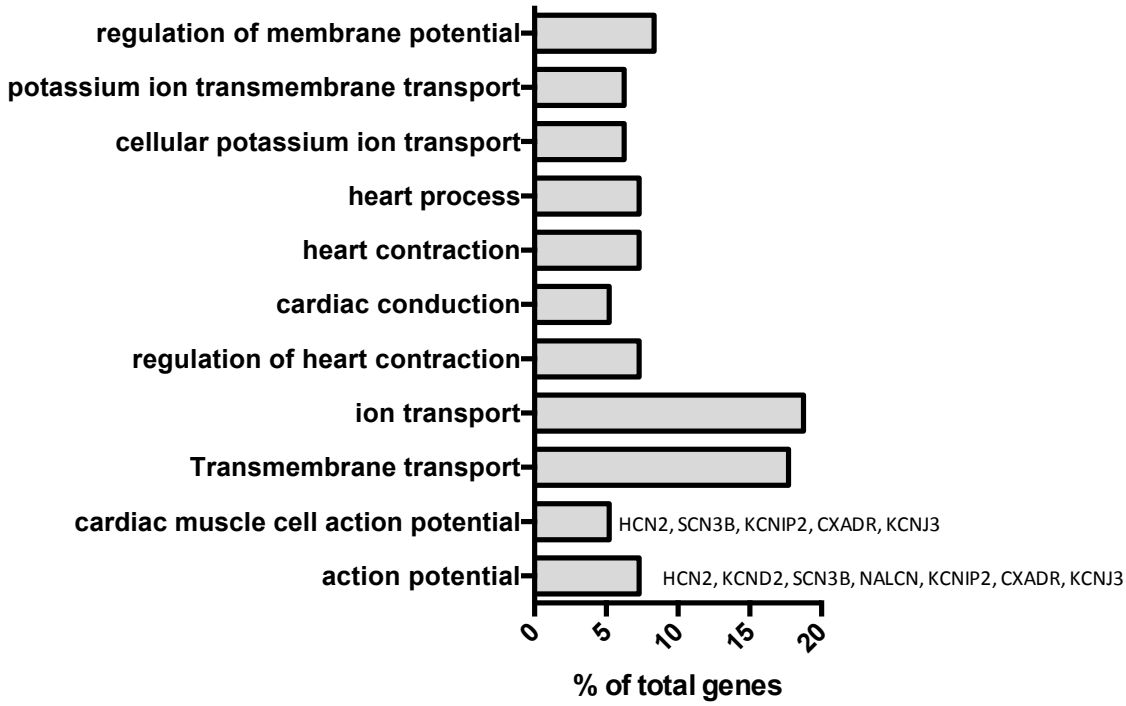

Figure 29. Gene ontology of 123 UP-regulated genes, in AAV-RAX2aeGFP treated rods

Biological processes enriched in rods after treatment with hRAX2aeGFP. Classes were sorted by false discovery rate (FDR), from bottom to top (higher to lower). Classes with FDR equal and/or lower than 0,05 were retained.

STRING analysis was performed on genes belonging in the action potential category to understand biological connections between these proteins. Biological interactions between four out seven of the analyzed genes were found (Figure 30).

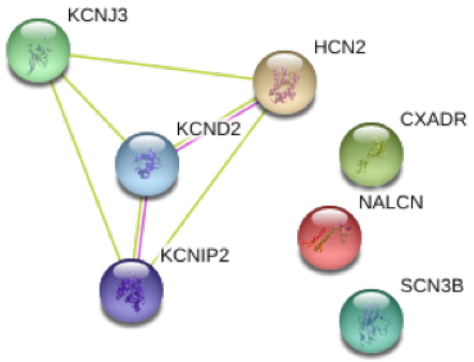

Figure 30 STRING protein-protein interaction analyses.

KCNJ3, KCND2, KCIPN2 and *HCN2* were part of synaptic transmission and regulation of membrane potential GO classes (Figure 31).

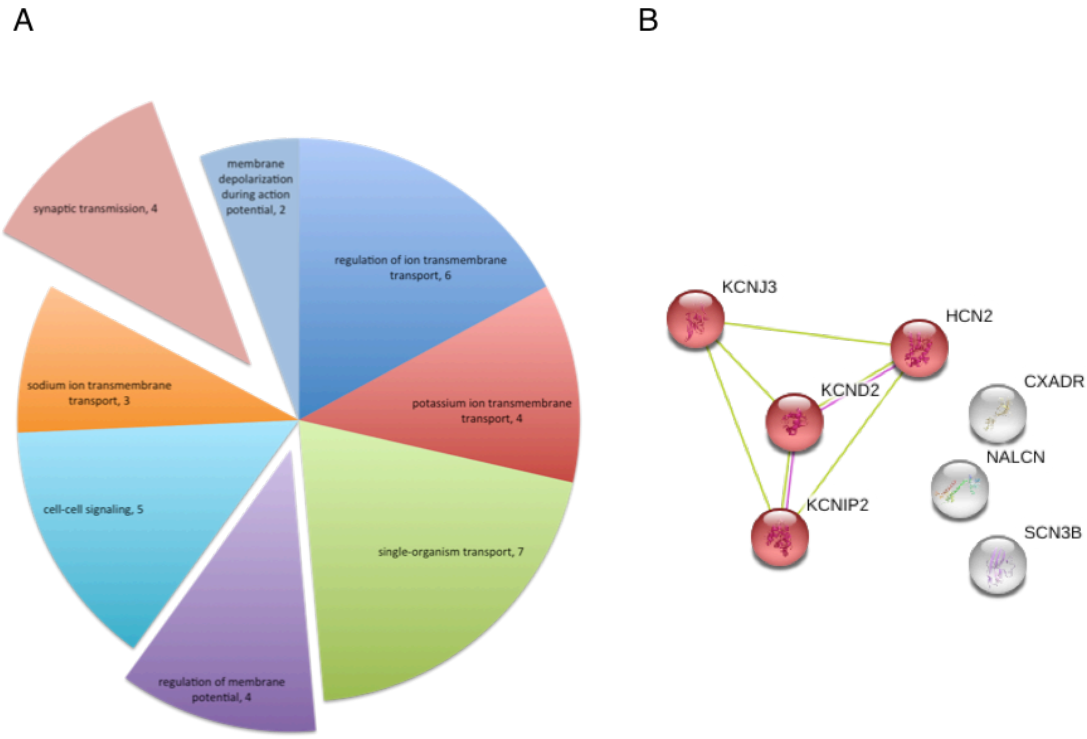

Figure 31 STRING: Gene ontology

(A) Pie chart showing distribution of BP in which KCNJ3, KCND2, HCN2 and KCNIP2 were involved. Classes in violet and light red retained all four genes. (B) Graphical representation of proteins belonging to synaptic transmission GO class (In red).

Considering that the DNA binding domain (from H136 to E195 in human) was totally conserved (100% identity) between human and porcine *RAX*, binding predictions using *RAX* position weight matrix were conducted on genes of action potential classes. *RAX* binding sites in the proximal promoter were found for six out of seven analyzed genes (*SCN3B, NALCN, CXADR, KCNIP2, KCNJ3, KCND2*) (Table 3). *HCN2* was excluded from the analysis due to its poor annotated promoter sequence in the porcine genome.

Gene	Core match	Matrix match	Sequence	Factor	Chromosome	Start	End	Strand	TSS_Position
SCN3B	1	0,863	atattTAATTcacctca	RAX	chr9	55820875	55820891	-	_446
SCN3B	1	0,898	cagaaccAATTAatcaa	RAX	chr9	55820771	55820787	-	-342
SCN3B	1	0,999	accAATTAat	RAX	chr9	55820774	55820783	-	-338
NALCN	1	0,996	ggcAATTAaa	RAX	chr11	77164634	77164643	+	-815
NALCN	0,901	0,875	agcagAAATTaacacaa	RAX	chr11	77165281	77165297	+	-168
CXADR	1	0,871	aagtgtgAATTAatgtg	RAX	chr13	192284317	192284333	+	-524
KCNIP2	0,901	0,887	aggagctAATTTaaggg	RAX	chr14	122727515	122727531	-	-1047
KCND2	0,899	0,866	gctctctAATTCgtcaa	RAX	chr18	28126890	28126906	-	-455
KCND2	1	0,87	tgcccTAATTgtgctga	RAX	chr18	28126315	28126331	-	120
KCNJ3	0,901	0.870	aggcattAATTTaaaaa	RAX	chr15	69329292	69329310	+	-423

Table 3 RAX binding sites on action potential genes

Binding prediction was performed on porcine sequences from -2000 to +500 bp relative to TSS. To direct the analysis RAX position weight matrix from transfac was used. Reported binding sites included in -1000 bp, + 200

Trying to clarify the effect of *RAX* on gene expression and to understand its GRN, intersection between DEGs in rods versus cones and RAX-treated rods versus untreated was made (Rod Vs Cone ∩ Rod-Rax Vs Rod) (Figure 32 A). Fifty-six genes were common between the two analyses, out of which 26 genes were up-regulated in both *RAX*-treated rods and in cones, demonstrating that

the expression of a cone-specific gene set was induced by the ectopic expression of *RAX* in rods (Figure 32 B).

Noteworthy, of the 26 genes three out of seven (*HCN2, KCNJ3* and *NALCN*) found enriched in action potential GO classes (Figure 29) were expressed both in cone and in rod transduced with *RAX* (Figure 33).

Furthermore also an important component of cone phototransduction cascade, cone opsin interacting alfa subunit of G protein known as GNAT2, was up regulated after the treatment with RAX in rods. Immunofluorescence confirmed *GNAT2* mis-localization in rods (Figure 34 A-B).

Binding prediction showed two putative sites in the porcine *GNAT2* proximal promoter region (between -750 and +1), and binding sites also in *KCNJ3* and *NALCN* promoter regions (Table 3 and 4).

Gene	Core match	Matrix match	Sequence	Factor	Chromosome	Start	End	Strand	TSS_Position
GNAT2	0.901	0.865	gctccAAATTagtttcc	RAX	chr4	120979864	120979888	+	-733
GNAT2	1.000	0.882	agggtTAATTtatccca	RAX	chr4	120981540	120981559	+	-27

Table 4 RAX predicted binding sites on GNAT2 promoter

Prediction was performed on GNAT2 with RAX position weight matrix on promoter region comprising -2000bp and +500bp relative to TSS.

Three genes (*HCN2, KCNJ3* and *NALCN*) out of the 7 from the GO, which cluster for action potential and ion transport classes belong to the cone-specific intersection (26 genes, Figure 32 A), confirming a presumptive importance of these genes in *RAX* GRN.

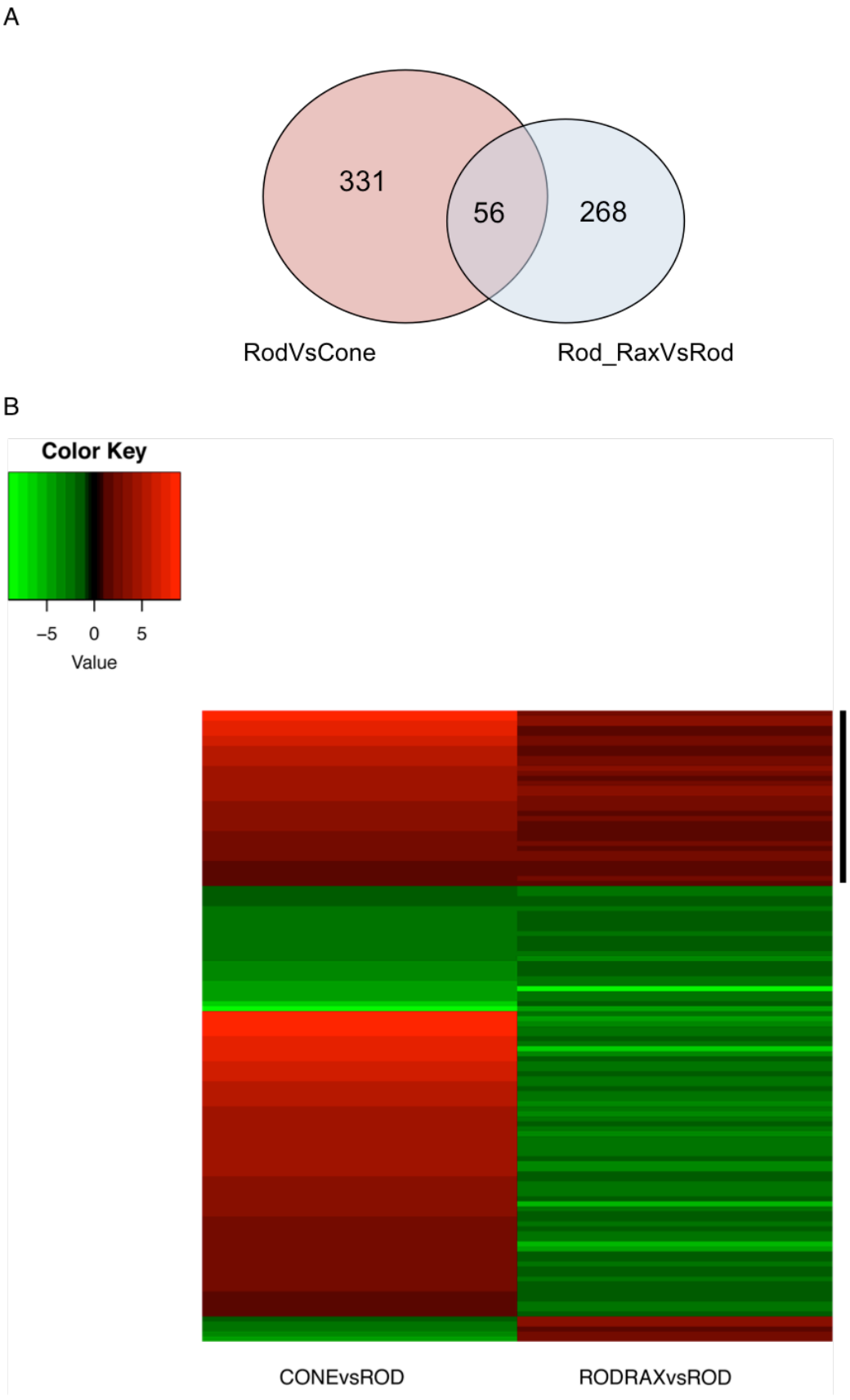

Figure 32 Intersection of Rod Vs Cone with Rod-Rax Vs Rod untreated

(A) Venn diagram shows common genes from the two groups of DE analysis. (B) Heat map shows differences in log fold change (logFC) between the two DE analyses. Genes Up regulated in both cones and RAX treated rods (26) were indicated with the black line. Color key gradient scale indicated up regulation in red and down regulation in green.

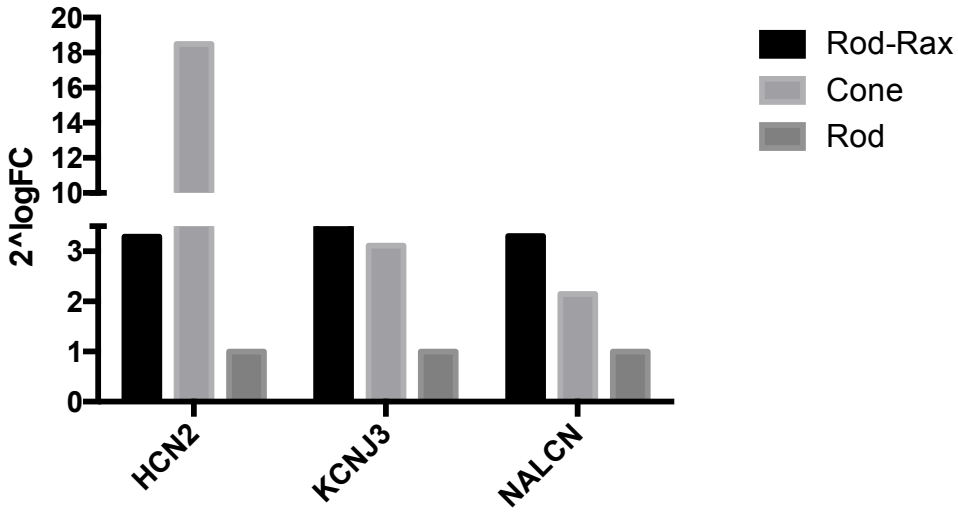

Figure 33 Fold change of expression level of HCN2, KCNJ3 and NALCN in rod-Rax, cone compared to untreated rod.

Fold change of HCN2, KCNJ3 and NALCN genes compared to rod basal expression. 2^log FC indicate the fold change calculated starting from normalized counts from RNA-sequencing

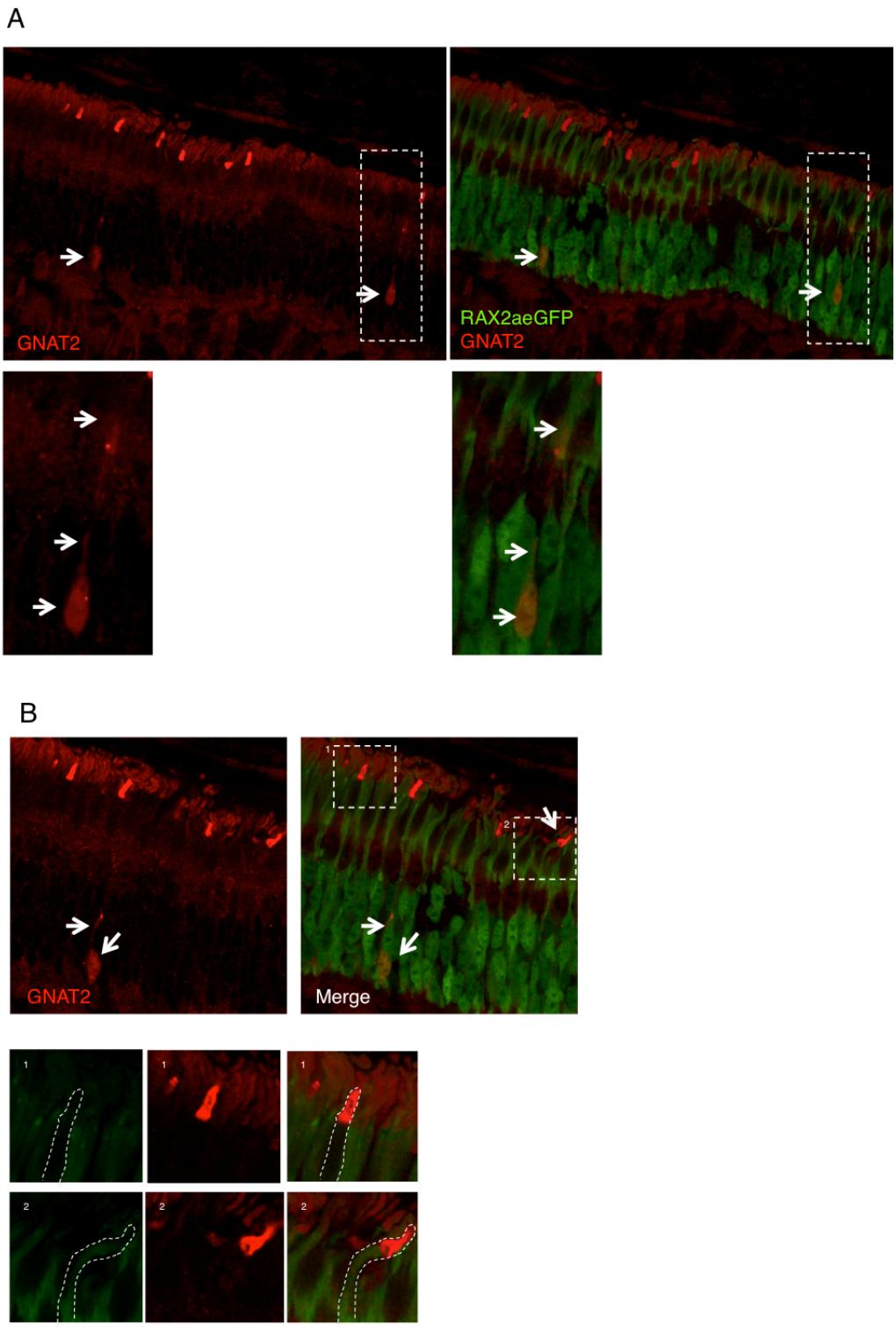

Figure 34 GNAT2 expression in rods

(A) GNAT2 expression in rods treated with AAV 2/8 hGNAT1-RAX-2a-eGFP. Arrows indicate GNAT2 localization in soma, inner and outer segment of rod cell. (B) Magnification showed co-localization of eGFP dye with GNAT2, in red (panel 2). Panel 1, showed cone cells un transduced with RAX, and the endogenous localization of GNAT2.

To better understand the effect of *Rax* over expression whole retinal ERGs were conducted fifteen days after subretinal injection of AAV2/8 hGNAT1-hRAX-2a-eGFP comparing the results to the contralateral eye injected with AAV2/8 hGNAT1-eGFP as control. From ERG, the scotopic b-wave (dark-adapted) was similar to that in the eGFP treated eye, while the mesopic (dark adapted) was found lower than in control and the photopic b-wave (light adapted) were higher in the RAX-treated eye compared to the eGFP control. Signals from flicker protocol were not significantly different between the two conditions (Figure 35), thus indicating that *Rax* expression in rods perturbs specific rod response properties.

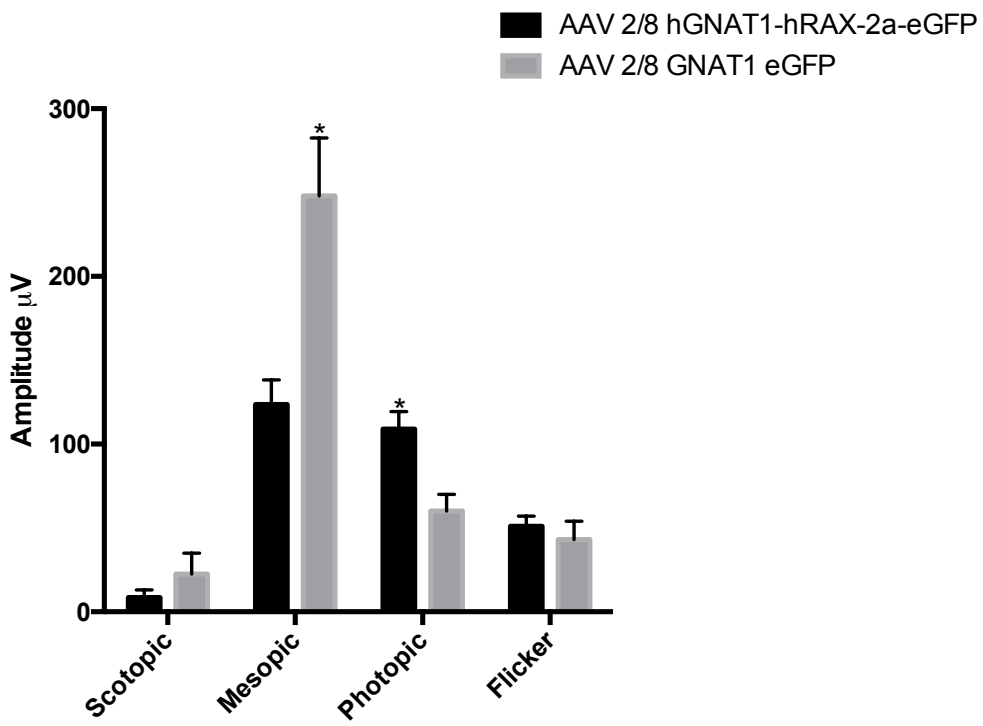

Figure 35 Mesopic and photopic alteration in rod treated with Rax

ERG analysis showed lower mesopic and higher photopic responses in rod treated with Rax transgene compared to contralateral eye. N= mean of 3 independent experiments; standard error calculated on mean values (SEM); * p value < 0,05 from student t test.

This result together with the binding predictions provided strong evidence that RAX was able to influence the expression of genes involved in regulation of light responses in rod background. Furthermore, binding predictions suggest a possible direct role of *RAX* in DNA binding and regulation of transcription of the analyzed genes in the context of a rod epigenomic background. Further analysis should be conducted to demonstrate the direct binding of *Rax* on predicted target genes. Furthermore, knock-down of *Rax* in cone cells may clarify the GRN of *RAX* under physiological conditions in the adult porcine retina. Furthermore these data shown that *RAX* may have an effect both on gene already expressed in rods and on genes normally expressed in cones and that this strongly correlates with an altered electrophysiological phenotype.

Discussion

Cells composing an individual organism share the same DNA sequence. Differences between cells and organs derive from a plethora of phenomena that occurs during development. DNA methylation, histone modifications, non-coding RNA (nc-RNA) regulation and different spatio-temporal expression of transcription factors activity generate differential gene expression.

The retina, an array of neuronal cells that convert light stimuli into signaling information for brain-mediated visual perception. The retina is a particularly suitable organ model to study its functions during development and in adulthood and correlate them to gene regulation (Pinelli *et al*, 2016; Whitmore *et al*, 2014; Farkas *et al*, 2013; Siegert *et al*, 2012; Macosko *et al*, 2015; Kim *et al*, 2008b). However, the connection between GRN and single cell functions is yet far from being known.

In this thesis, we used a strategy to compare the differences in gene expression of two functionally related cells, rod and cone PRs. We used somatic gene transfer with AAV vetcor to label and isolate rods and cones. The labeling strategy of PRs (double-Fluo) served for the selection of rod and cone single cell populations, which was then followed by RNA-sequencing. From mRNA profiling we identified using bioinformatics analysis and gene ontology eight-rod specific and eight-cone specific known and unknown TFs. Among them we selected a cone-specific TF, RAX, which was ectopically expressed in rods to study its GRN. The further transcriptome analysis of Rax transduced rods identified a gene set that may control a key aspect of PRs function such as the

membrane potential. Moreover, we integrated these RNA-seq data with functional data, using ERG analysis, showing an altered electrofunctional retina responses followed by RAX transduction, which are in accordance with the molecular findings.

In particular, the first part of my thesis was aimed at characterizing differentially expressed TFs and the GRNs controlling rod and cone functions, here studied in their fully differentiated status. I set up a method to select pure populations of rods and cones from the same porcine retina using single AAV8 vector administration. Cells transduced with AAV vector express eGFP and mCherry reporters in rods and mCherry in cones taking advantage of the use of GNAT1 and GRK1 promoter elements. With this “double fluo” strategy I was able to separate cone and rod populations, from the same retina, at the same time. I have shown how the double fluo strategy is effective to identify either rods or cones and that selected eGFP/mCherry and mCherry populations express typical markers of rods and cones, respectively. I compared the rod and cone transcriptomes with that of the whole retina to filter out all genes expressed not only in PRs but also in others type of cells composing the retina. Through bioinformatics analyses I found a presumptive molecular contamination of immune system related genes into cone dataset. These genes, including the microglial marker *Iba1,* were differentially expressed in cones compared to rod and retina. Using a co-expression data set, which was built-up in the laboratory for a different project, I found that the cone data were essentially formed by two different clusters of genes that were immune system and photoreceptorial

related, respectively. Through this analysis I selected a sub set of 128 cone specific genes, using these for the subsequent analyses. The reason of this immune system molecular contamination should be further investigated.

From the mRNA profiling, I have shown that cones and rods are characterized by different sets of genes serving the same biological functions, such as responses to light stimuli. Analyzing gene expression for TFs, I found 8 different TFs associated with rods and 8 with cones. In particular, I have shown that cones-specific TFs, *RAX*, *SALL3* and *SIX6*, that are known to be important during the development of neural retinal in mice (de Melo *et al*, 2011; Baba *et al*, 2011; Furukawa *et al*, 1997a) form a putative regulatory network co-controlling many genes, including the key *M-opsin* TF drivers Thyroid Hormone Receptor Beta (*THRB*; (Ng *et al*, 2001).

In the second part of my PhD thesis I tried to recapitulate the GRN of *RAX* in porcine retina, by ectopic expression of human *RAX* in rods by AAV8 vector gene transfer. Analyzing the gene ontology of up regulated genes, I found that *RAX* controls a set of genes having a role in PRs membrane potential (*HCN2*, *KCND2, SCN3B, NALCN, KCNIP2, CXADR, KCNJ3*). Furthermore, from mRNA profiling I found that 26 cone-specific genes were up regulated in rods after RAX transduction, demonstrating that, despite the fully differentiated state of rods, it is possible to activate expression of a cone gene set associated with a specific function. These results demonstrate that rods have the competence to express a discrete set of genes related to a specific function, governed by *RAX* (Oh *et al*, 2007; Montana *et al*, 2013). I found that many genes up-regulated after *RAX*

treatment in rods contain predicted binding sites in the proximal promoter region. In vitro and in vivo chromatin immunoprecipitation and functional validation will be necessary to confirm these predictions and to clarify direct targets of *RAX* in rods and thus in cones.

To correlate the *RAX* regulatory molecular findings, I analyzed the response to light of *RAX* transduced retina. From electrophysiological analysis, I found both lower mesopic (combined response of rod and cone) and higher photopic (isolated cones) responses in the *RAX*-treated eye compared to an eGFP-treated contralateral eye. These electrofunctional data may correlate with the up-regulation of genes, such as *HCN2* and *KNCJ3* that have a role in stabilizing the membrane potential through ionic influx, after light-mediated hyperpolarization. In particular, *HCN2* belong to the ion channel family of hyperpolarization-activated cyclic nucleotide-gated (HCN) cation channel that comprises four members (HCN1-4). Upon hyperpolarization, all four isoforms, following different kinetics, generate an inward current depolarizing the membrane (Ludwig *et al*, 1998; Santoro *et al*, 1998). I found that *HCN2* is expressed in cone cells of untreated porcine retina and is up regulated in rods after Rax treatment. From my data I can hypothesize that the rhythm of hyperpolarization-depolarization in rods treated with *RAX* is higher than in wt rods, due to the expression of both *HCN1* and *HCN2*. According to data on *HCN1* KO mouse, in which a sustained rod response was observed (Seeliger *et al*, 2011; Knop *et al*, 2008), the expression of these two channels by *RAX* in rods may generate both lower saturation of rods and a higher dynamic range of

cone responses, which may explain the electrophysiological findings. This "hyper-depo" hypothesis will be further studied.

References

Adams M, Dubnick M & Kerlavage A (1992) Sequence identification of 2, 375 human brain genes. *Nature* Available at: http://www.biology.iupui.edu/biocourses/Biol540/pdf/SeqID2375HumanGenes.pdf

Aguilar CA, Pop R, Shcherbina A, Watts A, Matheny RW, Cacchiarelli D, Han WM, Shin E, Nakhai SA, Jang YC, Carrigan CT, Gifford CA, Kottke MA, Cesana M, Lee J, Urso ML & Meissner A (2016) Transcriptional and Chromatin Dynamics of Muscle Regeneration after Severe Trauma. *Stem Cell Reports* **7:** 983–997 Available at: http://dx.doi.org/10.1016/j.stemcr.2016.09.009

Akimoto M, Cheng H, Zhu D, Brzezinski J a, Khanna R, Filippova E, Oh ECT, Jing Y, Linares J-L, Brooks M, Zareparsi S, Mears AJ, Hero A, Glaser T & Swaroop A (2006) Targeting of GFP to newborn rods by Nrl promoter and temporal expression profiling of flow-sorted photoreceptors. *Proc. Natl. Acad. Sci. U. S. A.* **103:** 3890–3895 Available at: http://www.pubmedcentral.nih.gov/articlerender.fcgi?artid=1383502&tool=pmcentrez&rendertype=abstract

Allocca M, Mussolino C, Garcia-Hoyos M, Sanges D, Iodice C, Petrillo M, Vandenberghe LH, Wilson JM, Marigo V, Surace EM & Auricchio A (2007) Novel adeno-associated virus serotypes efficiently transduce murine

photoreceptors. *J. Virol.* **81:** 11372–80 Available at: http://jvi.asm.org/content/81/20/11372.short

Auricchio A, Hildinger M, O'Connor E, Gao GP & Wilson JM (2001) Isolation of highly infectious and pure adeno-associated virus type 2 vectors with a single-step gravity-flow column. *Hum. Gene Ther.* **12:** 71–76

Baba Y, Iida A & Watanabe S (2011) Sall3 plays essential roles in horizontal cell maturation through regulation of neurofilament expression levels. *Biochimie* **93:** 1037–1046 Available at: http://dx.doi.org/10.1016/j.biochi.2011.02.016

Bailey TJ, El-Hodiri H, Zhang L, Shah R, Mathers PH & Jamrich M (2004) Regulation of development by Rx genes. *Int. J. Dev. Biol.* **48:** 761–770

Botta S, Marrocco E, de Prisco N, Curion F, Renda M, Sofia M, Lupo M, Carissimo A, Bacci ML, Gesualdo C, Rossi S, Simonelli F & Surace EM (2016) Rhodopsin targeted transcriptional silencing by DNA-binding. *Elife* **5:**

Boye SE, Alexander JJ, Boye SL, Witherspoon CD, Sandefer KJ, Conlon TJ, Erger K, Sun J, Ryals R, Chiodo VA, Clark ME, Girkin CA, Hauswirth WW & Gamlin PD (2012) The human rhodopsin kinase promoter in an AAV5 vector confers rod- and cone-specific expression in the primate retina. *Hum. Gene Ther.* **23:** 1101–15

Brzezinski JA & Reh TA (2015) Photoreceptor cell fate specification in

vertebrates. *Development* **142:** 3263–3273 Available at: http://www.ncbi.nlm.nih.gov/pubmed/26443631

Carl M, Loosli F & Wittbrodt J (2002) Six3 inactivation reveals its essential role for the formation and patterning of the vertebrate eye. *Development* **129:** 4057–4063

Carter-Dawson LD & LaVail MM (1979) Rods and cones in the mouse retina. II. Autoradiographic analysis of cell generation using tritiated thymidine. *J. Comp. Neurol.* **188:** 263–272

Cepko C (2014) Intrinsically different retinal progenitor cells produce specific types of progeny. *Nat. Rev. Neurosci.* **15:** 615–627 Available at: http://www.ncbi.nlm.nih.gov/pubmed/25096185%5Cnhttp://www.nature.com/doifinder/10.1038/nrn3767

Cepko CL (2015) The Determination of Rod and Cone Photoreceptor Fate. *Annu. Rev. Vis. Sci.* **1:** 211–234 Available at: http://www.annualreviews.org.gate1.inist.fr/doi/full/10.1146/annurev-vision-090814-121657

Chandler MJ, Smith PJ, Samuelson D a & MacKay EO (1999) Photoreceptor density of the domestic pig retina. *Vet. Ophthalmol.* **2:** 179–184 Available at: http://www.ncbi.nlm.nih.gov/pubmed/11397262%5Cnhttp://onlinelibrary.wiley.com/store/10.1046/j.1463-5224.1999.00077.x/asset/j.1463-

5224.1999.00077.x.pdf?v=1&t=gqca9scw&s=5400dfb3f971368858ee44ec77e082819894a791

Chen S, Wang QL, Nie Z, Sun H, Lennon G, Copeland NG, Gilbert DJ, Jenkins N a & Zack DJ (1997) Crx, a novel Otx-like paired-homeodomain protein, binds to and transactivates photoreceptor cell-specific genes. *Neuron* **19:** 1017–30 Available at: http://www.ncbi.nlm.nih.gov/pubmed/9390516

Cheng H, Khanna H, Oh ECT, Hicks D, Mitton KP & Swaroop A (2004) Photoreceptor-specific nuclear receptor NR2E3 functions as a transcriptional activator in rod photoreceptors. *Hum. Mol. Genet.* **13:** 1563–1575

Conesa A, Madrigal P, Tarazona S, Gomez-Cabrero D, Cervera A, McPherson A, Szczesniak MW, Gaffney DJ, Elo LL, Zhang X & Mortazavi A (2016) A survey of best practices for RNA-seq data analysis. *Genome Biol* **17:** 13 Available at: http://www.ncbi.nlm.nih.gov/pubmed/26813401

Curcio C, Sloan K, Kalina R & Hendrickson A (1990) Human photoreceptor topography. *J Comp Neurol.* **4:** 497–523

Dhallan SR, Macke JP, Eddy LR, Nathansi J, Shows B & Reed F (1992) Human Rod Photoreceptor cGMP-gated Channel: Amino Acid Sequence, Gene Structure, and Functional Expression. *J. Neurosci.* **12:** 3248–3256

Drittanti L, Rivet C, Manceau P, Danos O & Vega M (2000) High throughput production, screening and analysis of adeno-associated viral vectors. *Gene*

Ther **7:** 924–929 Available at: http://www.ncbi.nlm.nih.gov/entrez/query.fcgi?cmd=Retrieve&db=PubMed&dopt=Citation&list_uids=10849551

Dyer MA & Cepko CL (2001) Regulating proliferation during retinal development. *Nat. Rev. Neurosci.* **2:** 333–342

Dyka FM, Boye SL, Ryals RC, Chiodo VA, Boye SE & Hauswirth WW (2014) Cone specific promoter for use in gene therapy of retinal degenerative diseases. *Adv. Exp. Med. Biol.* **801:** 695–701

Farkas MH, Grant GR, White J a, Sousa ME, Consugar MB & Pierce E a (2013) Transcriptome analyses of the human retina identify unprecedented transcript diversity and 3.5 Mb of novel transcribed sequence via significant alternative splicing and novel genes. *BMC Genomics* **14:** 486 Available at: http://www.ncbi.nlm.nih.gov/pubmed/23865674

Feigenspan A, Janssen-Bienhold U, Hormuzdi S, Monyer H, Degen J, Söhl G, Willecke K, Ammermüller J & Weiler R (2004) Expression of connexin36 in cone pedicles and OFF-cone bipolar cells of the mouse retina. *J. Neurosci.* **24:** 3325–34 Available at: http://www.jneurosci.org/cgi/doi/10.1523/JNEUROSCI.5598-03.2004%5Cnhttp://www.ncbi.nlm.nih.gov/pubmed/15056712

Franze K, Grosche J, Skatchkov SN, Schinkinger S, Foja C, Schild D, Uckermann O, Travis K, Reichenbach A & Guck J (2007) Muller cells are

living optical fibers in the vertebrate retina. *Proc. Natl. Acad. Sci.* **104:** 8287–8292 Available at: http://www.pnas.org/cgi/doi/10.1073/pnas.0611180104

Fujitani Y, Fujitani S, Luo H, Qiu F, Burlison J, Long Q, Kawaguchi Y, Edlund H, MacDonald RJ, Furukawa T, Fujikado T, Magnuson MA, Xiang M & Wright C V (2006) Ptf1a determines horizontal and amacrine cell fates during mouse retinal development. *Development* **133:** 4439–4450 Available at: http://www.ncbi.nlm.nih.gov/pubmed/17075007

Fujiwara KT, Kataoka K & Nishizawa M (1993) Two new members of the maf oncogene family, mafK and mafF, encode nuclear b-Zip proteins lacking putative trans-activator domain. *Oncogene* **8:** 2371–2380 Available at: https://www.scopus.com/record/display.uri?eid=2-s2.0-0027249794&origin=inward&txGid=9C036BF0731E50ED62E1E8DDA241DFAF.wsnAw8kcdt7IPYLO0V48gA%3A2

Furukawa T, Kozak CA & Cepko CL (1997a) Rax, a Novel Paired-Type Homeobox Gene, Shows Expression in the Anterior Neural Fold and Developing Retina. *Proc. Natl. Acad. Sci.* **94:** 3088–3093 Available at: http://www.pnas.org/cgi/content/short/94/7/3088

Furukawa T, Morrow EM & Cepko CL (1997b) Crx, a novel otx-like homeobox gene, shows photoreceptor-specific expression and regulates photoreceptor differentiation. *Cell* **91:** 531–541

Furukawa T, Morrow EM, Li T, Davis FC & Cepko CL (1999) Retinopathy and attenuated circadian entrainment in Crx-deficient mice. *Nat. Genet.* **23:** 466–470

Goldman D (2014) Müller glial cell reprogramming and retina regeneration. *Nat. Rev. Neurosci.* **15:** 431–42 Available at: http://dx.doi.org/10.1038/nrn3723

Herrmann S, Schnorr S & Ludwig A (2015) Hcn channels???modulators of cardiac and neuronal excitability. *Int. J. Mol. Sci.* **16:** 1429–1447

Hrdlickova R, Toloue M & Tian B (2016) RNA-Seq methods for transcriptome analysis. *Wiley Interdiscip. Rev. RNA* **8:**

Irie S, Sanuki R, Muranishi Y, Kato K, Chaya T & Furukawa T (2015) Rax homeoprotein regulates photoreceptor cell maturation and survival in association with Crx in the postnatal mouse retina. *Mol. Cell. Biol.* **35:** MCB.00048-15

Jayaram H, Khaw PT, MacLaren RE & Limb GA (2012) Focus on Molecules: Neural retina leucine zipper (NRL). *Exp. Eye Res.* **104:** 99–100 Available at: http://dx.doi.org/10.1016/j.exer.2012.02.012

Khani SC, Pawlyk BS, Bulgakov O V., Kasperek E, Young JE, Adamian M, Sun X, Smith AJ, Ali RR & Li T (2007) AAV-mediated expression targeting of rod and cone photoreceptors with a human rhodopsin kinase promoter. *Investig. Ophthalmol. Vis. Sci.* **48:** 3954–3961

Kim DS, Matsuda T & Cepko CL (2008a) A Core Paired-Type and POU

Homeodomain-Containing Transcription Factor Program Drives Retinal Bipolar Cell Gene Expression. *J. Neurosci.* **28:** 7748–7764 Available at: http://www.jneurosci.org/cgi/doi/10.1523/JNEUROSCI.0397-08.2008

Kim DS, Ross SE, Trimarchi JM, Aach J, Greenberg ME & Cepko CL (2008b) Identification of molecular markers of bipolar cells in the murine retina. *J. Comp. Neurol.* **507:** 1795–810 Available at: http://www.pubmedcentral.nih.gov/articlerender.fcgi?artid=2665264&tool=pmcentrez&rendertype=abstract

Knop GC, Seeliger MW, Thiel F, Mataruga A, Kaupp UB, Friedburg C, Tanimoto N & Müller F (2008) Light responses in the mouse retina are prolonged upon targeted deletion of the HCN1 channel gene. *Eur. J. Neurosci.* **28:** 2221–2230

Lamb TD (2013) Evolution of phototransduction, vertebrate photoreceptors and retina. *Prog. Retin. Eye Res.* **36:** 52–119 Available at: http://dx.doi.org/10.1016/j.preteyeres.2013.06.001

Lee J, Myers C a, Williams N, Abdelaziz M & Corbo JC (2010) Quantitative fine-tuning of photoreceptor cis-regulatory elements through affinity modulation of transcription factor binding sites. *Gene Ther.* **17:** 1390–9 Available at: http://www.ncbi.nlm.nih.gov/pubmed/20463752

London A, Benhar I & Schwartz M (2013) The retina as a window to the brain-from eye research to CNS disorders. *Nat. Rev. Neurol.* **9:** 44–53 Available

at: http://www.ncbi.nlm.nih.gov/pubmed/23165340

Ludwig A, Zong X, Jeglitsch M, Hofmann F & Biel M (1998) A family of hyperpolarization-activated mammalian cation channels. *Nature* **393:** 587–591 Available at: http://www.nature.com/nature/journal/v393/n6685/full/393587a0.html

Macosko EZ, Basu A, Satija R, Nemesh J, Shekhar K, Goldman M, Tirosh I, Bialas AR, Kamitaki N, Martersteck EM, Trombetta JJ, Weitz DA, Sanes JR, Shalek AK, Regev A & McCarroll SA (2015) Highly Parallel Genome-wide Expression Profiling of Individual Cells Using Nanoliter Droplets. *Cell* **161:** 1202–1214 Available at: http://www.ncbi.nlm.nih.gov/pubmed/26000488

Marmor MF, Holder GE, Seeliger MW & Yamamoto S (2004) Standard for clinical electroretinography (2004 update). *Doc. Ophthalmol.* **108:** 107–114

Masland RH (2012) The Neuronal Organization of the Retina. *Neuron* **76:** 266–280 Available at: http://dx.doi.org/10.1016/j.neuron.2012.10.002

Mathers PH, Grinberg a, Mahon K a & Jamrich M (1997) The Rx homeobox gene is essential for vertebrate eye development. *Nature* **387:** 603–607

Mears a J, Kondo M, Swain PK, Takada Y, Bush R a, Saunders TL, Sieving P a & Swaroop a (2001) Nrl is required for rod photoreceptor development. *Nat. Genet.* **29:** 447–52 Available at: http://www.ncbi.nlm.nih.gov/pubmed/11694879

Mears AJ, Swaroop A, Williams DS & Jr ENP (2015) Features of the Photoreceptors of the Nrl Knockout Mouse. **46:** 2156–2167

de Melo J, Peng GH, Chen S & Blackshaw S (2011) The Spalt family transcription factor Sall3 regulates the development of cone photoreceptors and retinal horizontal interneurons. *Development* **138:** 2325–2336 Available at: http://www.ncbi.nlm.nih.gov/pubmed/21558380

Montana CL, Kolesnikov A V, Shen SQ, Myers C a, Kefalov VJ & Corbo JC (2013) Reprogramming of adult rod photoreceptors prevents retinal degeneration. *Proc. Natl. Acad. Sci. U. S. A.* **110:** 1732–7 Available at: http://www.pubmedcentral.nih.gov/articlerender.fcgi?artid=3562787&tool=pmcentrez&rendertype=abstract

Montana CL, Lawrence KA, Williams NL, Tran NM, Peng GH, Chen S & Corbo JC (2011) Transcriptional regulation of neural retina leucine zipper (Nrl), a photoreceptor cell fate determinant. *J. Biol. Chem.* **286:** 36921–36931

Morshedian A, Fain GL & Fain GL (2017) The evolution of rod photoreceptors.

Mueller C, Ratner D, Zhong L, Esteves-Sena M & Gao G (2012) Production and discovery of novel recombinant adeno-associated viral vectors. *Curr. Protoc. Microbiol.* **1:**

Muranishi Y, Terada K & Furukawa T (2012) An essential role for Rax in retina and neuroendocrine system development. *Dev. Growth Differ.* **54:** 341–348

Muranishi Y, Terada K, Inoue T, Katoh K, Tsujii T, Sanuki R, Kurokawa D,

Aizawa S, Tamaki Y & Furukawa T (2011) An essential role for RAX homeoprotein and NOTCH-HES signaling in Otx2 expression in embryonic retinal photoreceptor cell fate determination. *J Neurosci* **31:** 16792–16807 Available at: http://www.ncbi.nlm.nih.gov/pubmed/22090505

Mussolino C, della Corte M, Rossi S, Viola F, Di Vicino U, Marrocco E, Neglia S, Doria M, Testa F, Giovannoni R, Crasta M, Giunti M, Villani E, Lavitrano M, Bacci ML, Ratiglia R, Simonelli F, Auricchio a & Surace EM (2011) AAV-mediated photoreceptor transduction of the pig cone-enriched retina. *Gene Ther.* **18:** 637–45 Available at: http://www.pubmedcentral.nih.gov/articlerender.fcgi?artid=3131697&tool=pmcentrez&rendertype=abstract

Nathans J (1992) Rhodopsin: Structure, function and genetics. *Biochemistry* **31:** 4923–4930

Ng L, Hurley JB, Dierks B, Srinivas M, Saltó C, Vennström B, Reh T a & Forrest D (2001) A thyroid hormone receptor that is required for the development of green cone photoreceptors. *Nat. Genet.* **27:** 94–98

Oh ECT, Cheng H, Hao H, Jia L, Khan NW & Swaroop A (2008) Rod differentiation factor NRL activates the expression of nuclear receptor NR2E3 to suppress the development of cone photoreceptors. *Brain Res.* **1236:** 16–29

Oh ECT, Khan N, Novelli E, Khanna H, Strettoi E & Swaroop A (2007)

Transformation of cone precursors to functional rod photoreceptors by bZIP transcription factor NRL. *Proc. Natl. Acad. Sci.* **104:** 1679–1684 Available at: http://www.pubmedcentral.nih.gov/articlerender.fcgi?artid=1780067&tool=pmcentrez&rendertype=abstract

Omori Y, Katoh K, Sato S, Muranishi Y, Chaya T, Onishi A, Minami T, Fujikado T & Furukawa T (2011) Analysis of transcriptional regulatory pathways of photoreceptor genes by expression profiling of the Otx2-deficient retina. *PLoS One* **6:** 1–12

PENG G-H & CHEN S (2005) Chromatin immunoprecipitation identifies photoreceptor transcription factor targets in mouse models of retinal degeneration: New findings and challenges. *Vis. Neurosci.* **22:** 575–586 Available at: https://www.cambridge.org/core/article/div-class-title-chromatin-immunoprecipitation-identifies-photoreceptor-transcription-factor-targets-in-mouse-models-of-retinal-degeneration-new-findings-and-challenges-div/2E3B55A34C8531005223C8BD6491225E

Pinelli M, Carissimo A, Cutillo L, Lai CH, Mutarelli M, Moretti MN, Singh MV, Karali M, Carrella D, Pizzo M, Russo F, Ferrari S, Ponzin D, Angelini C, Banfi S & Di Bernardo D (2016) An atlas of gene expression and gene co-regulation in the human retina. *Nucleic Acids Res.* **44:** 5773–5784

Rapaport F, Khanin R, Liang Y, Pirun M, Krek A, Zumbo P, Mason CE, Socci ND & Betel D (2013) Comprehensive evaluation of differential gene

expression analysis methods for RNA-seq data. *Genome Biol* **14:** R95 Available at: http://dx.doi.org/10.1186/gb-2013-14-9-r95

Santoro B, Liu DT, Yao H, Bartsch D, Kandel ER, Siegelbaum SA & Tibbs GR (1998) Identification of a gene encoding a hyperpolarization-activated pacemaker channel of brain. *Cell* **93:** 717–729

Schena M, Shalon D, Davis RW, Brown PO, AUSUBEL FM, BELLANNECHANTEL C, COX DR, GREEN ED, HOFTE H, HWANG I, JARVIS P, KAWASAKI ES, LEGUEN L, MEYEROWITZ EM, MORTON NE, NEWMAN T, PRUITT RE, SCHENA M, SCHENA M, SCHENA M, et al (1995) Quantitative monitoring of gene expression patterns with a complementary DNA microarray. *Science* **270:** 467–70 Available at: http://www.ncbi.nlm.nih.gov/pubmed/7569999

Seeliger MW, Brombas A, Weiler R, Humphries P, Knop G, Tanimoto N & Muller F (2011) Modulation of rod photoreceptor output by HCN1 channels is essential for regular mesopic cone vision. *Nat Commun* **2:** 532 Available at: http://www.ncbi.nlm.nih.gov/pubmed/22068599

Shichida Y & Matsuyama T (2009) Evolution of opsins and phototransduction. *Philos. Trans. R. Soc. Lond. B. Biol. Sci.* **364:** 2881–2895

Siegert S, Cabuy E, Scherf BG, Kohler H, Panda S, Le YZ, Fehling HJ, Gaidatzis D, Stadler MB & Roska B (2012) Transcriptional code and disease map for adult retinal cell types. *Nat Neurosci* **15:** 487–95, S1-2

Available at: http://www.ncbi.nlm.nih.gov/pubmed/22267162

Sonia Tarazona & Fernando Garc a-Alcalde (2011) Di_erential expression in RNA-seq:a matter of depth. *Genome Res.*: 2213–2223 Available at: http://genome.cshlp.org/content/early/2011/09/07/gr.124321.111.full.pdf+html

Swaroop A, Kim D & Forrest D (2010) Transcriptional regulation of photoreceptor development and homeostasis in the mammalian retina. *Nat. Rev. Neurosci.* **11:** 563–576 Available at: http://www.ncbi.nlm.nih.gov/pubmed/20648062 [Accessed March 7, 2013]

Swaroop A, Xu JZ, Pawar H, Jackson A, Skolnick C & Agarwal N (1992) A conserved retina-specific gene encodes a basic motif/leucine zipper domain. *Proc. Natl. Acad. Sci. U. S. A.* **89:** 266–70 Available at: http://www.ncbi.nlm.nih.gov/pubmed/1729696

Terada K, Kitayama A, Kanamoto T, Ueno N & Furukawa T (2006) Nucleosome regulator Xhmgb3 is required for cell proliferation of the eye and brain as a downstream target of Xenopus rax/Rx1. *Dev. Biol.* **291:** 398–412

Trapani I, Puppo A & Auricchio A (2014) Vector platforms for gene therapy of inherited retinopathies. *Prog. Retin. Eye Res.* **43:** 108–128

Tsuchiya M, Misaka R, Nitta K & Tsuchiya K (2015) Transcriptional factors, Mafs and their biological roles. *World J. Diabetes* **6:** 175–83 Available at: http://www.pubmedcentral.nih.gov/articlerender.fcgi?artid=4317310&tool=p

mcentrez&rendertype=abstract

Tsukamoto Y, Morigiwa K, Ueda M & Sterling P (2001) Microcircuits for night vision in mouse retina. *J. Neurosci.* **21:** 8616–23 Available at: http://www.ncbi.nlm.nih.gov/pubmed/11606649

Turner DL & Cepko CL (1987) A common progenitor for neurons and glia persists in rat retina late in development. *Nature* **328:** 131–136

Velculescu V, Zhang L, Vogelstein B & Kinzler KW (1995) Serial analysis of gene expression. *Science (80-.).* **270:** 484–487 Available at: http://www.sciencemag.org/cgi/content/abstract/sci;270/5235/484

Wang X, Xu S, Rivolta C, Li LY, Peng GH, Swain PK, Sung CH, Swaroop A, Berson EL, Dryja TP & Chen S (2002) Barrier to autointegration factor interacts with the cone-rod homeobox and represses its transactivation function. *J. Biol. Chem.* **277:** 43288–43300

Wang Z, Gerstein M & Snyder M (2009) RNA-Seq: a revolutionary tool for transcriptomics. *Nat. Rev. Genet.* **10:** 57–63 Available at: http://www.pubmedcentral.nih.gov/articlerender.fcgi?artid=2949280&tool=pmcentrez&rendertype=abstract

White MA, Kwasnieski JC, Myers CA, Shen SQ, Corbo JC & Cohen BA (2016) A Simple Grammar Defines Activating and Repressing cis-Regulatory Elements in Photoreceptors. *Cell Rep.* **17:** 1247–1254 Available at: http://dx.doi.org/10.1016/j.celrep.2016.09.066

Whitmore SS, Wagner AH, DeLuca AP, Drack A V., Stone EM, Tucker BA, Zeng S, Braun TA, Mullins RF & Scheetz TE (2014) Transcriptomic analysis across nasal, temporal, and macular regions of human neural retina and RPE/choroid by RNA-Seq. *Exp. Eye Res.* **129:** 93–106 Available at: http://dx.doi.org/10.1016/j.exer.2014.11.001

Young JE, Vogt T, Gross KW & Khani SC (2003) A short, highly active photoreceptor-specific enhancer/promoter region upstream of the human rhodopsin kinase gene. *Investig. Ophthalmol. Vis. Sci.* **44:** 4076–4085

Young RW (1967) The renewal of photoreceptor cell outer segments. *J. Cell Biol.* **33:** 61–72